Ann. Inst. H. Poincaré D
Comb. Phys. Interact. 12 (2025), 819–868
DOI 10.4171/AIHPD/205

Positive del Pezzo geometry

Nick Early, Alheydis Geiger, Marta Panizzut, Bernd Sturmfels, and Claudia He Yun

Abstract. Real, complex, and tropical algebraic geometry join forces in a new branch of mathematical physics called positive geometry. We develop the positive geometry of del Pezzo surfaces and their moduli spaces, viewed as very affine varieties. Their connected components are derived from polyhedral spaces with Weyl group symmetries. We study their canonical forms and scattering amplitudes, and we solve the likelihood equations.

1. Introduction

It has been known for two centuries that a cubic surface contains 27 lines. If the surface is obtained by blowing up six real points in $\mathbb{P}^2$, then the surface and its 27 lines are real. We consider the very affine cubic surface obtained by removing the 27 lines. That *real* surface has 130 connected components, namely, 10 triangles, 90 quadrilaterals, and 30 pentagons. This appears in our Theorem 3.1. The *complex* surface has Euler characteristic 90, as shown in Lemma 4.3. This is the number of solutions to the equations known as likelihood equations in statistics and as scattering equations in physics. The *tropical* surface is a balanced polyhedral complex which has the cograph of the Schläfli graph at infinity. This is the 10-regular graph with 27 vertices that records intersections among the 27 lines; see [36].

This article studies moduli of del Pezzo surfaces through the lens of positive geometry [2, 3]. It builds on work of Sekiguchi and Yoshida [37–39] and Hacking, Keel, and Tevelev [25]. Positive geometry highlights the trinity of real, complex, and tropical geometry. We saw this for the cubic surface in the previous paragraph, and we next summarize other main results.

Let $Y(3,n)$ denote the moduli space of configurations of n points in general position in the complex projective plane $\mathbb{P}^2$. For us, this means that no three points are collinear and no six lie on a conic. When $n \leq 7$, the space $Y(3,n)$ parametrizes marked del Pezzo surfaces of degree $9-n$ as the blow-up of $\mathbb{P}^2$ at the n points. From $Y(3,8)$,

Mathematics Subject Classification 2020: 05E14 (primary); 14J81, 14P99 (secondary).
Keywords: positive geometry, del Pezzo surface, scattering amplitude.

one obtains the moduli space by requiring that the eight points are not on a cubic that is singular at one of the points.

The Euler characteristics of $Y(3,6)$ and $Y(3,7)$ over $\mathbb{C}$ were recently computed in [7, 8] by means of cohomological methods. We here present an alternative derivation.

Theorem 4.1. *The Euler characteristic of the* complex *moduli space* $Y(3,n)$ *is* 32 *for* $n = 6$*, and it is* 3600 *for* $n = 7$*. For* $n = 8$*, a numerical computation gives* 4884387 *as a lower bound for the Euler characteristic.*

Theorem 8.1. *The* real *moduli space* $Y(3,6)$ *has* 432 *connected components, all* $W(E_6)$ *equivalent, and the closure of each is homeomorphic as a cell-complex to a simple* 4*-polytope with f-vector* $(45, 90, 60, 15)$*. The real moduli space* $Y(3,7)$ *has* 60480 *connected components, all* $W(E_7)$ *equivalent, and the closure of each is homeomorphic as a cell-complex to a simple* 6*-dimensional homology ball with f-vector* $(579, 1737, 2000, 1105, 297, 34)$.

These complex and real results complement those on *tropical* moduli spaces in [35, 36]. For instance, it is known that the tropicalization of $Y(3,6)$ is a simplicial fan with f-vector $(76, 630, 1620, 1215)$. The identification of the components in Theorem 8.1 and the transitive Weyl group action are due to Sekiguchi and Yoshida [37,39]. Our contribution is a combinatorial study of these objects, which we call *pezzotopes*. Also new are their f-vectors. We use the term pezzotope for two objects: the $W(E_n)$-equivalent connected components of $Y(3,n)$, for $n = 6, 7$; and in the case of $Y(3,6)$, the polytope that is homeomorphic to those components. We add the word "curvy" to emphasize that we are referring to the components.

One motivation for studying the real moduli spaces $Y(3,n)$ comes from physics. We aim to show that the pezzotopes are positive geometries in the sense of [2, 3]. This involves identifying the canonical form and the resulting scattering amplitude. In Sections 8 and 9, we compute the scattering amplitude for the E_6 pezzotope, see equation (8.4), and a system of perfect u-equations, in the sense of [5, 27], see equation (8.3). For $n = 7$, see Theorem 9.4.

Figure 1 depicts the E_6 pezzotope. It offers a colorful illustration of Theorems 8.1 and 8.2. Our final highlights concern the formal definition of positive geometry by Arkani-Hamed, Bai, and Lam [3, 30], which stipulates the existence of a canonical differential form Ω like (2.5). We prove this for $Y(3,6)$ and conjecture it for $Y(3,7)$.

Theorem 10.5. *The moduli space* $Y(3,6)$ *is a positive geometry for any of its* 432 *regions, each of which is a curvy* E_6 *pezzotope.*

In Theorem 10.6, we single out one of these 432 regions, denoted by $Y_+(3,6)$ and called the positive moduli space of del Pezzo surfaces, and we provide a parametrization for it.

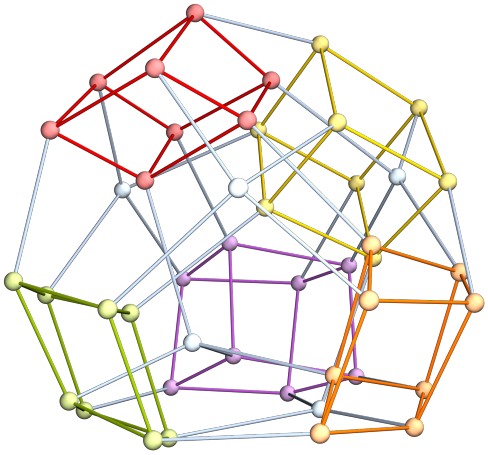

Figure 1. The real moduli space $Y(3,6)$ is glued from 432 copies of a simple 4-polytope with $f = (45, 90, 60, 15)$. The picture shows its edge graph. The amplitude is a rational function, given as the sum of 45 reciprocal monomials, one for each vertex. Singularities correspond to facets: five cubes (in color) and ten associahedra. The Weyl group $W(E_6)$ acts on this data.

We now define concepts that are used throughout the paper, starting with a realization of $Y(3,n)$ as a very affine variety, i.e., as a closed subvariety of an algebraic torus. Homogeneous coordinates for the n points are the columns of a $3 \times n$ matrix whose 3×3 minors p_{ijk} are nonzero. The condition for six points to lie on a conic is the vanishing of the Plücker binomial

$$q = p_{134}p_{156}p_{235}p_{246} - p_{135}p_{146}p_{234}p_{256}. \tag{1.1}$$

Two matrices represent the same configuration if and only if they differ by left multiplication with $\mathrm{GL}(3,\mathbb{C})$ and by scaling the columns with an element in the torus $(\mathbb{C}^*)^n$. Therefore, by fixing a projective basis, every configuration in $Y(3,n)$ is represented by a unique matrix:

$$M = \begin{bmatrix} 1 & 0 & 0 & 1 & 1 & 1 & \cdots & 1 \\ 0 & 1 & 0 & 1 & x_{1,1} & x_{1,2} & \cdots & x_{1,n-4} \\ 0 & 0 & 1 & 1 & x_{2,1} & x_{2,2} & \cdots & x_{2,n-4} \end{bmatrix}. \tag{1.2}$$

We note that $Y(3,n)$ is a subset of the familiar space $X(3,n)$ of configurations in linearly general position. Namely, $Y(3,n)$ is obtained from $X(3,n)$ by removing the $\binom{n}{6}$ divisors of the form q. The space $X(3,n)$ was studied in detail in [1]. Both $Y(3,n)$ and $X(3,n)$ are very affine varieties of dimension $2n-8$, by (1.2), and they have appeared in the physics literature [17, 21].

For $n = 6$ and $n = 7$, we also employ the parametrization used in [25, 34, 36], where the points lie on a cuspidal cubic. After an automorphism of $\mathbb{P}^2$, we can thus choose

$$M = \begin{bmatrix} 1 & 1 & 1 & 1 & \cdots & 1 \\ d_1 & d_2 & d_3 & d_4 & \cdots & d_n \\ d_1^3 & d_2^3 & d_3^3 & d_4^3 & \cdots & d_n^3 \end{bmatrix}. \tag{1.3}$$

The 3×3 minors and the conic conditions factor into linear forms $d_i - d_j$, $d_i + d_j + d_k$, and $d_{i_1} + d_{i_2} + d_{i_3} + d_{i_4} + d_{i_5} + d_{i_6}$. These are the roots of type E_6 and E_7. They define arrangements of 36 hyperplanes in $\mathbb{P}^5$ and 63 hyperplanes in $\mathbb{P}^6$. The complements of these arrangements are the moduli spaces for 6 and 7 points in general position together with a cuspidal cubic through them. Our moduli spaces are embedded in $\mathbb{P}^{39}$ and $\mathbb{P}^{134}$ by certain monomials in these linear forms of degree 9 and 7, respectively. This yields the *Yoshida variety* [35, (6.2)] and the *Göpel variety* [34, Section 6], on which the Weyl groups act by permuting coordinates.

This paper is structured as follows. In Section 2, we perform a case study on $Y(3, 5)$. We will generalize this analysis to $Y(3, 6)$ and $Y(3, 7)$ in the rest of the paper. In Section 3, we consider the real del Pezzo surfaces $\mathcal{S}_n^\circ$, and we characterize their polygonal regions for $n = 5, 6$, as summarized in Theorem 3.1. In Section 4, we pass to the complex setting and we determine the Euler characteristics of both $\mathcal{S}_{n-1}^\circ$ and $Y(3, n)$ for $n = 6, 7$. Section 5 applies numerical methods for computing the Euler characteristic. Tropical likelihood degenerations [1, Section 8] are applied to verify theoretical results and offer new insights. In Section 6, we study the parametrizations (1.3) of the del Pezzo moduli spaces via the reflection hyperplane arrangements E_6 and E_7. This centers around the Yoshida variety and the Göpel variety. Section 7 connects our findings with the physics literature on scattering amplitudes.

In Sections 8 and 9, we define the pezzotopes, compute their f-vectors, and present their perfect u-equations. The line arrangements in Figure 3 and the graphs in Figure 4 reveal remarkable structures that are of independent interest for Weyl group combinatorics. Theorem 9.4 characterizes the E_7 pezzotope, and it offers a view from commutative algebra.

In Section 10, we derive the regions of $Y(3, n)$ from Grassmannians and their tropicalizations. The chirotopes in Theorem 10.4 offer a fresh perspective on positive Grassmannians. The residues of the canonical form Ω for Theorem 10.5 match the $10 + 5$ facets in Figure 1.

This article relies heavily on software and data. These materials are made available in the `MathRepo` collection at MPI-MiS via https://mathrepo.mis.mpg.de/positive-delPezzo.

2. Blowing up four points

This section is a warm-up for the rest of the paper. It offers a case study of the surface $\mathcal{S}_4$, which is obtained by blowing up $\mathbb{P}^2$ at four points in general position. We present an elementary proof that $\mathcal{S}_4^\circ$ is a *positive geometry* in the sense of Arkani-Hamed, Bai, and Lam [3]; i.e., each region of the real surface has a canonical differential form which satisfies the recursive axioms in [30, Section 2]. Such regions are *worldsheet associahedra* [2, Figure 18].

Without loss of generality, the four points to be blown-up are $(1:0:0)$, $(0:1:0)$, $(0:0:1)$, and $(1:1:1)$. These points span six lines. The very affine surface $\mathcal{S}_4^\circ$ is the complement of these lines in $\mathbb{P}^2$. Namely, $\mathcal{S}_4^\circ$ consists of all points $(1:x:y)$ such that

$$xy(1-x)(1-y)(y-x) \neq 0. \tag{2.1}$$

The following well-known fact highlights that this example is of wide interest.

Proposition 2.1. *The very affine surface defined by* (2.1) *plays various roles:*

$$\mathcal{S}_4^\circ = Y(3,5) = X(3,5) = X(2,5) = \mathcal{M}_{0,5}.$$

The surface $\mathcal{S}_4$ is the tropical compactification of $\mathcal{M}_{0,5}$, as seen in [31, Section 6.5].

We conclude that our del Pezzo surface $\mathcal{S}_4^\circ$ also plays the role of a moduli space in two different ways. It is the moduli space $\mathcal{M}_{0,5}$ of five distinct labeled points on the line $\mathbb{P}^1$, and it is also the moduli space $Y(3,5)$ of del Pezzo surfaces of degree four. This double casting of $Y(3,5)$—it acts as a del Pezzo surface and as a moduli space of del Pezzo surfaces—is our motivation for dedicating an entire section to this seemingly minor actor. In the trinity of geometries, adulated in the Introduction, the pictures for $Y(3,5)$ are as follows.

- The complex surface $\mathcal{S}_\mathbb{C}$ has Euler characteristic 2. [1, Figure 1]
- The real surface $\mathcal{S}_\mathbb{R}$ consists of 12 pentagons. [24, Figure 11]
- The tropical surface $\mathcal{S}_\mathbb{T}$ is the cone over the Petersen graph. [36, Figure 3]

The Euler characteristic of $\mathcal{S}_\mathbb{C}$ is the number of critical points of the log-likelihood function:

$$L = s_1\log(x) + s_2\log(y) + s_3\log(1-x) + s_4\log(1-y) + s_5\log(y-x). \tag{2.2}$$

See [22, Section 6] and [28, Theorem 1]. The coefficients s_i are parameters. These are known as Mandelstam invariants in physics, and they represent the data in algebraic statistics; see [41]. There are two critical points, obtained as the solutions of the likelihood equations

$$\frac{s_1}{x} - \frac{s_3}{1-x} - \frac{s_5}{y-x} = \frac{s_2}{y} - \frac{s_4}{1-y} + \frac{s_5}{y-x} = 0. \tag{2.3}$$

We can solve this in radicals, thanks to the quadratic formula. If the s_i are positive, then each of the two bounded regions of (2.1) contains one critical point. For the tropical setting, where the parameters s_i are in the valued field $\mathbb{R}\{\{\varepsilon\}\}$, we refer to [1, Section 7].

When interpreting our surface as $\mathcal{M}_{0,5}$, we write its points as 2×5 matrices

$$M = \begin{bmatrix} 1 & 1 & 1 & 1 & 0 \\ 0 & x & y & 1 & 1 \end{bmatrix}.$$

The 10 maximal minors p_{ij} of the matrix M are the linear expressions in (2.1) and (2.3), namely,

$$\begin{aligned}(p_{12}, p_{13}, p_{14}, p_{15}, p_{23}, p_{24}, p_{25}, p_{34}, p_{35}, p_{45}) \\ = (x, y, 1, 1, y - x, 1 - x, 1, 1 - y, 1, 1).\end{aligned}$$

As in [2, (6.7)] and [14, (2.6)], we use five cross ratios as coordinates on $\mathcal{M}_{0,5}$:

$$u_1 = \frac{p_{25}p_{34}}{p_{35}p_{24}} = \frac{1-y}{1-x}, \quad u_2 = \frac{p_{13}p_{45}}{p_{14}p_{35}} = y, \quad u_3 = \frac{p_{24}p_{15}}{p_{14}p_{25}} = 1-x,$$
$$u_4 = \frac{p_{35}p_{12}}{p_{13}p_{25}} = \frac{x}{y}, \quad u_5 = \frac{p_{14}p_{23}}{p_{13}p_{24}} = \frac{y-x}{(1-x)y}.$$

Following [5, (3)], the u-coordinates satisfy the following quadratic equations:

$$u_1u_3 + u_2 = u_2u_4 + u_3 = u_3u_5 + u_4 = u_4u_1 + u_5 = u_5u_2 + u_1 = 1. \quad (2.4)$$

These equations give an embedding of $\mathcal{M}_{0,5}$ as a closed subvariety of the torus $(\mathbb{C}^*)^5$.

To appreciate the beauty of the Laurent polynomial ideal in (2.4), consider its real solutions. Among the $64 = 2^5$ possible sign patterns for $(u_1, u_2, u_3, u_4, u_5)$, precisely 12 are realized:

$$\begin{array}{cccccc} (+\,+\,+\,+\,+) & (-\,+\,+\,+\,+) & (+\,-\,+\,+\,+) & (+\,+\,-\,+\,+) & (+\,+\,+\,-\,+) & (+\,+\,+\,+\,-) \\ (-\,-\,-\,-\,-) & (+\,-\,+\,-\,+) & (+\,+\,-\,+\,-) & (-\,+\,+\,-\,+) & (+\,-\,+\,+\,-) & (-\,+\,-\,+\,+) \end{array}$$

These sign vectors label the 12 regions in $\mathcal{S}_{\mathbb{R}}$, all of which are the same up to symmetry. We focus on the region $(+\,+\,+\,+\,+)$, where the following tropical equations are valid:

$$\begin{aligned}\min(u_1 + u_3, u_2) = \min(u_2 + u_4, u_3) = \min(u_3 + u_5, u_4) \\ = \min(u_4 + u_1, u_5) = \min(u_5 + u_2, u_1) = 0.\end{aligned}$$

The solution to these equations is the cone over a pentagon. This is one of the 12 pentagons in the Petersen graph of $\mathcal{S}_{\mathbb{T}}$. To see the pentagon classically in $\mathcal{S}_{\mathbb{R}}$, we note that (2.4) implies $0 \le u_1, u_2, u_3, u_4, u_5 \le 1$. If u_i is 0, then both neighboring variables u_{i-1} and u_{i+1} must be 1, and the remaining two variables are nonnegative and sum

to 1. This reveals the pentagon. In other words, the set of nonnegative solutions to (2.4) is a curvy pentagon in $(\mathbb{R}_+)^5 \subset (\mathbb{C}^*)^5$.

We are now prepared to prove that this curvy pentagon is a positive geometry by showing that the canonical form for $\mathcal{M}_{0,5}$ is the following 2-form:

$$\begin{aligned}\Omega &= d\log\left(\frac{u_2u_5}{u_1}\right) \wedge d\log\left(\frac{u_4}{u_3u_5}\right) \\ &= d\log\left(\frac{y-x}{1-y}\right) \wedge d\log\left(\frac{x}{1-y}\right) = \frac{\mathrm{d}x\,\mathrm{d}y}{x(x-y)(1-y)}.\end{aligned} \tag{2.5}$$

On the line $u_2 = 0$, we have $u_1 = u_3 = 1$ and $u_4 + u_5 = 1$. The residue of Ω on that line is $d\log(u_4/u_5) = d\log(u_4/(1-u_4))$, which is the canonical form of the line segment. A similar calculation works for the residues at the other four boundaries $u_i = 0$. Since line segments are positive geometries, we thus verify the recursive axioms in [3, Section 2.1]. By symmetry, each curvy pentagon endows the surface $\mathcal{M}_{0,5}$ with the structure of a positive geometry.

We compute the *scattering amplitude* of $\mathcal{M}_{0,5}$ following [20, (2.12)]. To integrate Ω, we write $\mathcal{H}_L$ for the Hessian of the function (2.2), and we sum $\det(\mathcal{H}_L^{-1})x^{-2}(x-y)^{-2}(1-y)^{-2}$ over the two solutions of (2.3). The result is the amplitude

$$\frac{1}{s_1s_4} + \frac{1}{s_4(s_3+s_4+s_5)} + \frac{1}{(s_3+s_4+s_5)s_5} + \frac{1}{s_5(s_1+s_2+s_5)} + \frac{1}{(s_1+s_2+s_5)s_1}. \tag{2.6}$$

Our discussion illustrates the aim of this article: extending the study of $\mathcal{S}_{\mathbb{C}}$, $\mathcal{S}_{\mathbb{R}}$, $\mathcal{S}_{\mathbb{T}}$ to del Pezzo surfaces of degree $9-n$ and their moduli spaces $Y(3,n)$ for larger n.

3. Polygons

In this section, we examine polygonal decompositions of real del Pezzo surfaces. We denote the blow-up of $\mathbb{P}^2$ at n general real points, as described in the introduction, by the *del Pezzo surface* $\mathcal{S}_n$. The anticanonical divisor of such a surface is very ample for $n \leq 6$. Its sections are cubics that vanish at the n points in $\mathbb{P}^2$, and these give an embedding of $\mathcal{S}_n$ into $\mathbb{P}^{9-n}$. With this notation, $\mathcal{S}_6$ is a cubic surface in $\mathbb{P}^3$. The surface $\mathcal{S}_5$ lives in $\mathbb{P}^4$, where it is an intersection of two quadrics. For $n = 4, 5, 6$, the surface contains 10, 16, 27 straight lines. For $n = 7$, the anticanonical map is 2-to-1 from $\mathcal{S}_7$ onto $\mathbb{P}^2$. Its branch locus is a quartic curve Q. There are 56 exceptional curves on $\mathcal{S}_7$, and these are mapped onto the 28 bitangents of Q.

The very affine surfaces $\mathcal{S}_n^\circ$ result from removing the 10, 16, 27, 56 lines from $\mathcal{S}_n$. The lines are denoted as in [36]. We write F_{ij} for the line in $\mathbb{RP}^2$ spanned by the points i and j, and E_i for the exceptional divisor over the point i. For $n \geq 6$, let G_I be the unique conic through the five points labeled by $\{1, 2, \ldots, n\} \setminus I$. For $n = 7$, we

denote by H_i the unique cubic that passes through all seven points and has a node at point i.

We will study the connected components of $\mathcal{S}_n^\circ$, here called *polygons*, with focus on their shapes and numbers. Each polygon is bounded by a subset of the lines. The *face vector* $f = (v, e, p)$ records the number v of vertices, the number e of edges, and the number p of polygons in this polygonal subdivision of $\mathcal{S}_n$. The subdivision for $n = 4$ consists of 12 pentagons, and it has

$$f = (15, 30, 12).$$

We summarize the situation in the following theorem. Here, a del Pezzo surface is called *general* if every point is contained in at most two lines.

Theorem 3.1. *The subdivision of any general real del Pezzo surface $\mathcal{S}_n$ has* 36, 130, 806 *polygons for $n = 5, 6, 7$. For $n = 5$, it has* 20 *quadrilaterals and* 16 *pentagons, and the f-vector is* (40, 80, 36). *Each line is incident to* 5 *quadrilaterals and* 5 *pentagons. For $n = 6$, there are* 10 *triangles,* 90 *quadrilaterals, and* 30 *pentagons, and the f-vector is* (135, 270, 130). *Twelve of the* 27 *lines on $\mathcal{S}_6$ are disjoint from the triangles, and these form a Schläfli double-six. Each of the other* 15 *lines is incident to* 2 *triangles,* 12 *quadrilaterals, and* 6 *pentagons.*

Proof. Consider a polygonal subdivision of a closed surface, with v vertices, e edges, and p polygons. The Euler characteristic of the surface satisfies

$$\chi = v - e + p.$$

If the surface is $\mathcal{S}_n$, i.e., the blow-up of $\mathbb{RP}^2$ at n general points, then $\chi = 1 - n$. The number of (-1)-curves on $\mathcal{S}_n$ is 10, 16, 27, 56 for $n = 4, 5, 6, 7$. We call these "lines", in spite of $\mathbb{RP}^1$ being a circle.

Each line is incident to the same number of other lines, and that number is 3, 5, 10, 28. For $n \leq 6$, the intersection of two lines on $\mathcal{S}_n$ is either empty or a single point. For $n = 7$, however, each line meets one of the lines twice, and it meets 27 other lines at one point.

It follows that the number of edges in the subdivision is the product of the number of lines and the number of incident lines. We hence find that e equals 30, 80, 270, 1624. The number of vertices is half the number of edges; i.e., $v = e/2$ equals 15, 40, 135, 812. From this data, we compute the number p of polygons in each case with the formula

$$p = \frac{e}{2} + \chi.$$

Therefore, the number of polygons equals $p = 12, 36, 130, 806$ for $n = 4, 5, 6, 7$.

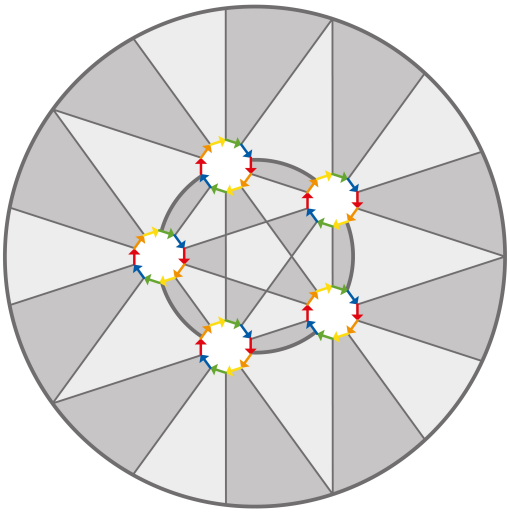

Figure 2. Subdivision of the del Pezzo surface $\mathcal{S}_5$ into 20 quadrilaterals (dark) and 16 pentagons (light). Each blown-up point is replaced by a decagon with opposite sides identified.

To get more refined information, we discuss each case separately. For $n = 4$, this was done in Section 2 where we referred to the work of Devadoss [24] on $\mathcal{M}_{0,n}$ over $\mathbb{R}$. For $n = 5$, we offer Figure 2. After a projective transformation, we may assume that the five points are in convex position, so the conic G that passes through these points is an ellipse. The arrangement of ten lines $F_{12}, F_{13}, \ldots, F_{45}$ and the conic G divides $\mathbb{RP}^2$ into 36 regions, and we color them by light gray and dark gray in the checkerboard pattern shown in Figure 2. The blow-up replaces the point i by a projective line E_i, which in the figure is obtained from a decagon by double-covering. Arrows with the same color are identified, and they create new edges in the gray regions. Considering these new colorful edges, each of the 16 light gray regions is a pentagon, and each of the 20 dark gray regions is a quadrilateral.

We now turn to $n = 6$. Rather than pointing to a picture, we leave the job to a computer. The input is a random element in $Y(3, 6)$, that is, a random configuration of six points in $\mathbb{RP}^2$. We identify the regions in $\mathbb{RP}^2$ created by removing the 15 lines $F_{12}, F_{13}, \ldots, F_{56}$ and the six conics $G_1, G_2, G_3, G_4, G_5, G_6$. For each region that is incident to a point i, we identify the 10 new colorful edges created by the circle E_i. The output of the computation is a list of tuples of lines, each delineating one of the 130 polygons. An explicit list is shown in Example 3.2. From this data, we can read off interesting properties. Recall that the cubic surface $\mathcal{S}_6$ has 36 double-sixes. We found that there is a unique double-six that is disjoint from the 10 triangular regions. This is identified in the data below. ∎

Example 3.2. Fix the cubic surface $\mathcal{S}_6$ obtained from $\mathbb{P}^2$ by blowing up the six points in

$$M = \begin{bmatrix} -2 & 24 & 16 & 27 & 14 & 1 \\ -25 & 3 & 28 & 13 & 5 & 7 \\ -26 & -4 & 1 & -14 & 9 & 6 \end{bmatrix}.$$

The resulting subdivision of $\mathcal{S}_6$ has the ten triangles

$$E_4F_{24}G_2,\quad E_4F_{34}G_3,\quad E_5F_{15}G_1,\quad E_5F_{25}G_2,\quad E_6F_{16}G_1,$$
$$E_6F_{36}G_3,\quad F_{14}F_{25}F_{36},\quad F_{14}F_{26}F_{35},\quad F_{15}F_{26}F_{34},\quad F_{16}F_{24}F_{35}.$$

The 90 quadrilaterals are

$$E_1E_5G_3G_4,\ E_1E_5G_3G_6,\ E_1E_6F_{16}G_5,\ E_1E_6G_2G_4,\ E_1E_6G_2G_5,\ E_1E_6G_3G_4,$$
$$E_1F_{12}F_{14}F_{36},\ E_1F_{12}F_{14}G_1,\ E_1F_{12}F_{15}F_{36},\ E_1F_{13}F_{14}G_1,\ E_1F_{13}F_{16}F_{25},$$
$$E_1F_{15}F_{36}G_6,\ E_1F_{16}F_{25}G_5,\ E_2E_4G_1G_5,\ E_2E_4G_1G_6,\ E_2E_4G_3G_6,$$
$$E_2E_5F_{25}G_4,\ E_2E_5G_1G_6,\ E_2E_5G_3G_4,\ E_2E_5G_3G_6,\ E_2F_{12}F_{25}F_{34},$$
$$E_2F_{12}F_{26}F_{34},\ E_2F_{12}F_{26}G_2,\ E_2F_{15}F_{23}F_{24},\ E_2F_{15}F_{24}G_5,\ E_2F_{23}F_{26}G_2,$$
$$E_2F_{25}F_{34}G_4,\ E_3E_4G_1G_5,\ E_3E_4G_1G_6,\ E_3E_4G_2G_5,\ E_3F_{24}F_{36}G_4,$$
$$E_4F_{14}F_{23}F_{45},\ E_3F_{13}F_{24}F_{36},\ E_3F_{13}F_{35}G_3,\ E_3F_{16}F_{23}F_{34},\ E_3F_{16}F_{23}F_{35},$$
$$E_3F_{16}F_{34}G_6,\ E_3F_{23}F_{35}G_3,\ E_3E_6G_2G_4,\ E_3E_6G_2G_5,\ E_4F_{14}F_{23}F_{46},$$
$$E_4F_{14}F_{45}G_4,\ E_4F_{14}F_{46}G_4,\ E_4F_{24}F_{45}G_4,\ E_4F_{34}F_{46}G_4,\ E_5F_{12}F_{35}F_{45},$$
$$E_5F_{12}F_{35}F_{56},\ E_5F_{12}F_{45}G_2,\ E_5F_{15}F_{56}G_5,\ E_5F_{35}F_{45}G_5,\ E_5F_{35}F_{56}G_5,$$
$$E_6F_{13}F_{26}F_{46},\ E_6F_{13}F_{26}F_{56},\ E_6F_{13}F_{56}G_1,\ E_6F_{26}F_{46}G_6,\ E_6F_{26}F_{56}G_6,$$
$$E_6F_{36}F_{46}G_6,\ F_{12}F_{14}F_{56}G_1,\ F_{12}F_{15}F_{36}F_{46},\ F_{12}F_{25}F_{34}F_{46},\ F_{12}F_{26}F_{35}F_{45},$$
$$F_{12}F_{26}F_{45}G_2,\ F_{13}F_{14}F_{26}F_{56},\ F_{13}F_{14}F_{56}G_1,\ F_{13}F_{16}F_{24}F_{45},\ F_{13}F_{16}F_{25}F_{45},$$
$$F_{13}F_{24}F_{36}F_{45},\ F_{13}F_{25}F_{36}F_{45},\ F_{13}F_{35}F_{46}G_3,\ F_{14}F_{23}F_{35}F_{46},\ F_{14}F_{25}F_{46}G_4,$$
$$F_{15}F_{23}F_{24}F_{56},\ F_{15}F_{23}F_{34}F_{56},\ F_{15}F_{24}F_{56}G_5,\ F_{15}F_{26}F_{46}G_6,\ F_{15}F_{36}F_{46}G_6,$$
$$F_{16}F_{23}F_{34}F_{56},\ F_{16}F_{25}F_{45}G_5,\ F_{16}F_{34}F_{56}G_6,\ F_{23}F_{26}F_{45}G_2,\ F_{23}F_{35}F_{46}G_3,$$
$$F_{24}F_{35}F_{56}G_5,\ F_{24}F_{36}F_{45}G_4,\ F_{25}F_{34}F_{46}G_4,\ E_3F_{24}G_2G_4,\ E_2F_{34}G_3G_4,$$
$$E_2F_{15}G_1G_5,\ E_1F_{25}G_2G_5,\ E_3F_{16}G_1G_6,\ E_1F_{36}G_3G_6.$$

Finally, the 30 pentagons are

$$E_1E_5F_{12}F_{15}G_1,\ E_1E_5F_{15}G_1G_6,\ E_1E_5F_{25}G_2G_4,\ E_1E_6F_{13}F_{16}G_1,$$
$$E_1F_{13}F_{14}F_{25}F_{36},\ E_2E_4F_{23}F_{24}G_2,\ E_2E_4F_{24}G_2G_5,\ E_2E_5F_{12}F_{25}G_2,$$
$$E_2F_{15}F_{23}F_{26}F_{34},\ E_3E_4F_{23}F_{34}G_3,\ E_3E_4F_{34}G_3G_6,\ E_3E_6F_{13}F_{36}G_3,$$
$$E_3E_6F_{16}G_1G_5,\ E_3E_6F_{36}G_3G_4,\ E_3F_{13}F_{16}F_{24}F_{35},\ E_4F_{23}F_{24}F_{45}G_2,$$

$E_4F_{23}F_{34}F_{46}G_3$, $E_5F_{12}F_{15}F_{56}G_1$, $E_5F_{25}F_{45}G_2G_5$, $E_6F_{13}F_{36}F_{46}G_3$, $E_6F_{16}F_{56}G_1G_6$, $F_{12}F_{14}F_{25}F_{36}F_{46}$, $F_{12}F_{14}F_{26}F_{35}F_{56}$, $F_{12}F_{15}F_{26}F_{34}F_{46}$, $F_{13}F_{14}F_{26}F_{35}F_{46}$, $F_{14}F_{23}F_{26}F_{35}F_{45}$, $F_{14}F_{25}F_{36}F_{45}G_4$, $F_{15}F_{26}F_{34}F_{56}G_6$, $F_{16}F_{23}F_{24}F_{35}F_{56}$, $F_{16}F_{24}F_{35}F_{45}G_5$.

We note that the following 12 symbols do not appear among the triangles:

$$\begin{array}{cccccc} E_1 & E_2 & E_3 & F_{45} & F_{46} & F_{56} \\ F_{23} & F_{13} & F_{12} & G_6 & G_5 & G_4 \end{array} \quad \rightarrow \quad \begin{array}{cccccc} 5 & 4 & 6 & 5 & 5 & 5 \\ 7 & 6 & 6 & 4 & 4 & 3 \end{array}$$

These 12 lines form a double-six. On the right we list the numbers of pentagons bounded by each line. Each of the other 15 lines bounds 2 triangles, 12 quadrilaterals, and 6 pentagons.

Remark 3.3. The Weyl group $W(E_n)$ acts on our data for $n = 6, 7$. Each group is generated by permuting the labels $1, 2, \ldots, n$ of $E_.$, $F_{..}$, $G_{..}$, $H_.$ plus one additional involution that represents the Cremona transformation of $\mathbb{P}^2$ centered at the triangle $E_1E_2E_3$. For $n = 6$, this Cremona involution equals

$$(E_1F_{23})(E_2F_{13})(E_3F_{12})(G_4F_{56})(G_5F_{46})(G_6F_{45}).$$

For $n = 7$, it is

$$(E_1F_{23})(E_2F_{13})(E_3F_{12})(G_{12}H_3)(G_{13}H_2)(G_{23}H_1)(F_{45}G_{67})(F_{46}G_{57})(F_{47}G_{56}) \times (F_{56}G_{47})(F_{57}G_{46})(F_{67}G_{45}).$$

Remark 3.4. Each triangle on the cubic surface S_6 shares its three edges with pentagons, and its vertices are adjacent to quadrilaterals. For instance, in the list above, the triangle $E_4F_{24}G_2$ shares its edges with the pentagons $E_2E_4F_{23}F_{24}G_2$, $E_2E_4F_{24} \times G_2G_5$, $E_4F_{23}F_{24}F_{45}G_2$. Its vertices are adjacent to the quadrilaterals $E_3E_4G_2G_5$, $E_3F_{24}G_2G_4$, $E_4F_{24}F_{45}G_4$. If we move around in the moduli space $Y(3, 6)$, then the triangle gets inverted when passing through an Eckardt divisor. This inversion replaces the pentagons with quadrilaterals and vice versa. In particular, the numbers 10, 90, and 30 of triangles, quadrilaterals, and pentagons remain the same when we cross the Eckardt divisor within a connected component of $Y(3, 6)$.

Example 3.5 (Clebsch cubic). A prominent surface is the Clebsch cubic, with 10 Eckhardt points. It is obtained by blowing up $\mathbb{P}^2$ at the vertices of a regular pentagon and its midpoint. Its subdivision consists of 120 quadrilaterals. Nearby in $Y(3, 6)$, as the Eckhardt points become triangles, their three adjacent quadrilaterals become pentagons.

To find the subdivisions of $\mathcal{S}_6$ and $\mathcal{S}_7$, we fix ternary forms for all exceptional curves apart from the E_i. We then compute the stratification of $\mathbb{R}^3$ that is given by signs $+$ or $-$ of these ternary forms. Each region in $\mathbb{R}^3$ is labeled by a sign vector of length 21 or length 49, respectively, for $n = 6, 7$. For the cubic surface ($n = 6$), this computation yields 260 sign vectors. Each of them labels a unique connected component in $\mathbb{R}^3$. The quotient map from $\mathbb{R}^3$ to $\mathbb{P}^2$ thus creates 130 polygons. The only remaining task is to weave in the exceptional curves E_i. This is done by hand, using a careful local analysis.

We now turn to the case $n = 7$. New phenomena arise because seven cubic curves are needed for subdividing $\mathbb{P}^2$. The polygonal subdivision of the surface $\mathcal{S}_7$ is created by the 7 exceptional divisors E_i, the 21 lines F_{ij}, the 21 conics G_{ij}, and the 7 cubics H_j. While removal of a single F_{ij} leaves $\mathbb{P}^2$ connected and removal of G_{ij} creates two connected components, it is important to note that removal of H_i divides $\mathbb{P}^2$ into three connected components. The analogous computation in $\mathbb{R}^3$ as above for $n = 6$ now yields 1596 distinct sign vectors. This is less than the number $1612 = 2 \cdot 806$, which is expected from Theorem 3.1. We believe that this discrepancy arises from the tripartition of $\mathbb{P}^2$ by nodal cubics. This deserves further study.

4. Euler characteristic

We now turn to the complex geometry of very affine varieties. The Euler characteristic is the key invariant. For statisticians, it yields the maximum likelihood (ML) degree [22]. For physicists, it counts the master integrals of a Feynman diagram [10, Section 3].

The Euler characteristic of the configuration space $X(3, n)$ equals $26, 1272, 188112$ for $n = 6, 7, 8$. This result is shown in [21] via soft limits and in [1] via stratified fibrations. In what follows, we determine the analogous numbers for moduli of del Pezzo surfaces, via the method of stratified fibrations. After the completion of this work, we learned that the same results had been proven in [7, 8] via cohomological methods. We know from Section 2 that

$$Y(3, 5) = X(3, 5)$$

has Euler characteristic 2.

Theorem 4.1. *The Euler characteristic of $Y(3, n)$ equals* $32,\ 3600$ *for $n = 6, 7$. The Euler characteristic of $Y(3, 8)$ is bounded below by* 4884387.

In this section, we offer formal proofs for $n = 6, 7$. These build on [1, Section 2]. The case $n = 8$ will be treated in Section 5. For a detailed explanation, see Experiment 5.2.

Remark 4.2. Olof Bergvall has computed the Euler characteristic of $Y(3,8)$ to be 4884480 via a finite-field method. This computation and its proof will appear in his upcoming paper.

We begin by calculating the Euler characteristics of very affine del Pezzo surfaces.

Lemma 4.3. *The general surfaces $\mathcal{S}_5^\circ$ and $\mathcal{S}_6^\circ$ have Euler characteristic* 16 *and* 90*, respectively. If the cubic surface has ℓ Eckhardt points, then its Euler characteristic drops to* $90-\ell$.

Proof. The complex projective plane $\mathbb{CP}^2$ has Euler characteristic $\chi = 3$. That number increases by 1 whenever we blow up one point. Hence, the compact surface $\mathcal{S}_n$ has $\chi = 3+n$. We pass to $\mathcal{S}_n^\circ$ by inclusion-exclusion. The Riemann sphere $\mathbb{CP}^1$ has $\chi = 2$, so we subtract 2 for each line, and we add 1 for each intersection point of two lines. For $n = 5$, we remove 16 lines and we add in 40 points, so we get

$$\chi = 8 - 16 \cdot 2 + 40 = 16.$$

For $n = 6$, we remove 27 lines and we add in 135 points, so we get

$$\chi = 9 - 27 \cdot 2 + 135 = 90.$$

We subtract 1 for each Eckhardt point, i.e., each point where three lines meet. ∎

Proof of Theorem 4.1. We consider the map $\pi_n : Y(3,n) \to Y(3,n-1)$ given by deleting the last point. For $n \leq 6$, this map is a fibration, with each fiber isomorphic to $\mathcal{S}_{n-1}^\circ$. Euler characteristic is multiplicative under fibrations. We know from Lemma 4.3 that $\mathcal{S}_5^\circ$ has $\chi = 16$. This implies that the Euler characteristic of $Y(3,6)$ is equal to $16 \cdot 2 = 32$.

We now turn to $n = 7$. The map π_7 is not a fibration but only a stratified fibration. This is analogous to [1, Section 5], and we apply the same technique. Namely, we identify all strata in $Y(3,6)$ and the fiber over each stratum, we compute the Euler characteristic for each piece, we analyze the poset structure of the stratification, and we use [1, Lemma 2.3].

The stratification of $Y(3,6)$ is given by the labels of Eckardt points on the cubic surface, i.e., triples of concurrent lines. In the blow-up picture, we see two types of Eckardt points.

- The 15 triples of lines F_{ij}, F_{kl}, F_{mn}, which we denote by $(ij)(kl)(mn)$.
- The 30 triples $E_i F_{ij} G_j$, where line F_{ij} is tangent to conic G_j at the point i in $\mathbb{P}^2$.

These 45 triples specify the tritangent planes of the general cubic surface. The Weyl group $W(E_6)$ acts transitively on the 45 triples. By [9], Table 1 summarizes the possible configurations of Eckardt points. They also show the poset structure on the strata.

EckPts	Representative Configuration	Strata
1	(16)(25)(34)	45
2	(16)(25)(34), (15)(26)(34)	270
3	(16)(25)(34), (15)(24)(36), (14)(26)(35)	240
4	(16)(25)(34), (15)(24)(36), (14)(26)(35), (15)(26)(34)	720
6	(16)(25)(34), (15)(26)(34), (12)(35)(46), (12)(36)(45), (13)(24)(56), (14)(23)(56)	540
9	(16)(25)(34), (14)(26)(35), (15)(24)(36), Q_{13}, Q_{46}, Q_{32}, Q_{65}, Q_{21}, Q_{54}	40
10	(16)(25)(34), (15)(24)(36), (14)(26)(35), (15)(26)(34), Q_{14}, Q_{16}, Q_{24}, Q_{36}, Q_{25}, Q_{35}	216
18	(14)(25)(36), (14)(26)(35), (15)(24)(36), (15)(26)(34), (16)(24)(35), (16)(25)(34), Q_{12}, Q_{13}, Q_{21}, Q_{23}, Q_{31}, Q_{32}, Q_{45}, Q_{46}, Q_{54}, Q_{56}, Q_{64}, Q_{65}	40

Table 1. All 2111 strata in $Y(3, 6)$, grouped by number of Eckardt points. Data from [9, Lemma 10] were verified in `Julia` using `OSCAR`. Column 3 lists the number of strata per type.

Table 1 is the del Pezzo variant of [1, Table 3]. We will compute $\chi(Y(3, 7))$ by using [1, Lemma 2.3], which we rewrite just like in [1, (16)]. In our setting, this takes the form

$$\chi(Y(3,7)) = \chi(Y(3,6)) \cdot \chi(F_{Y(3,6)}) - \sum_{S \in \mathbb{S}} \chi(S) \cdot \rho(S), \tag{4.1}$$

where $\mathbb{S}$ is the poset of 2111 strata, and

$$\rho(S) = \sum_{S' \in \mathbb{S}, S' \supseteq S} \mu(S, S') \cdot (\chi(F_{Y(3,6)}) - \chi(F_{S'})).$$

By Lemma 4.3, the generic fiber $F_{Y(3,6)}$ has $\chi = 90$, so the product on the left is $32 \cdot 90 = 2880$.

To prove Theorem 4.1, we must show that $\sum_{S \in \mathbb{S}} \chi(S) \cdot \rho(S) = -720$. By analyzing the poset of strata, we find that the analog of [1, Theorem 5.4] holds in our case: $\rho(T) = 1$ for the top stratum with one Eckardt point, and $\rho(S) = 0$ for all lower-dimensional strata S. There are 45 top strata T. They are all isomorphic. It remains

to show that $\chi(T) = -720/45 = -16$. Consider the map $\pi_6 : T \to Y(3,5)$ which deletes point 6.

We stratify $Y(3,5)$ as follows.

(1) Type a. General position.

(2) Type b_1. The three points $\overline{12} \cap \overline{34}$, $\overline{14} \cap \overline{23}$, and 5 are collinear.

(3) Type b_2. The three points $\overline{12} \cap \overline{34}$, $\overline{13} \cap \overline{24}$, and 5 are collinear.

(4) Type c. Setting $S = \overline{12} \cap \overline{34}$, the line $\overline{5S}$ is tangent to the conic through the five points.

The poset structure is simple: b_1, b_2, and c are pairwise disjoint and contained in a. For the fiber to have Eckardt point (12)(34)(56), point 6 must be on the line $\overline{5S}$ but retain general linear and quadratic position with the five points. We see that the fiber over a is $F_a = \mathbb{P}^1 \setminus \{7 \text{ points}\}$ and hence $\chi(F_a) = -5$. Similarly, for $u \in \{b_1, b_2, c\}$, we have $F_u = \mathbb{P}^1 \setminus \{6 \text{ points}\}$ and hence $\chi(F_u) = -4$. For the strata in $Y(3,5) = \mathcal{M}_{0,5}$, we find $\chi(a) = 2$ and $\chi(u) = -2$ for $u \in \{b_1, b_2, c\}$. Using [1, Lemma 2.3] again, we conclude that $\chi(T) = 2 \cdot (-5) - 3 \cdot (-2) \cdot 1 \cdot (-5 - (-4)) = -16$. ∎

We now examine the set-theoretic difference between $X(3,n)$ and $Y(3,n)$. For $n = 6$, this difference consists of configurations of six points in $\mathbb{P}^2$ in general linear position but lying on a conic. This is isomorphic to $\mathcal{M}_{0,6}$, which is reflected in the Euler characteristics:

$$\chi(X(3,6) \setminus Y(3,6)) = \chi(X(3,6)) - \chi(Y(3,6)) = 26 - 32 = -6 = \chi(\mathcal{M}_{0,6}). \quad (4.2)$$

For $n = 7$, the situation is more complicated. The boundary of $Y(3,7)$ in $X(3,7)$ consists of seven isomorphic strata $a_1, \ldots, a_7$, where a_i is the locus where the points $\{1, 2, \ldots, 7\} \setminus \{i\}$ are on a conic. Their pairwise intersection is the stratum $b \simeq \mathcal{M}_{0,7}$, where all points are on a conic. We have $\chi(b) = 24$. The following result is found by a stratified fibration. We omit the proof, which is analogous to but lengthier than the proof of Theorem 4.1.

Proposition 4.4. *The Euler characteristic* $\chi(a_7) = -312$.

The $n = 7$ analog to (4.2) is the following identity among Euler characteristics:

$$\begin{aligned} \chi(X(3,7) \setminus Y(3,7)) &= 1272 - 3600 = 7 \cdot (-312) - 6 \cdot 24 \\ &= \sum_{i=1}^{7} \chi(a_i) - 6\chi(b). \end{aligned} \quad (4.3)$$

In this section, we explored the complex geometry of some very affine varieties of interest. We showed how their Euler characteristics can be derived by means of inclusion-exclusion.

5. Numerical experiments

We now turn to the numerical solution of likelihood equations. See (2.3) for a tiny example. In this section, each item is labeled as Experiment to highlight the experimental nature of our investigation. Our computation yields a lower bound for the Euler characteristic for $Y(3,8)$.

A complex variety X is *very affine* if it is a closed subvariety of an algebraic torus $(\mathbb{C}^*)^m$. The *log-likelihood function* on X is the logarithm of a monomial with unknown exponents:

$$\log\bigl(z_1^{s_1} z_2^{s_2} \cdots z_m^{s_m}\bigr) = s_1 \log(z_1) + s_2 \log(z_2) + \cdots + s_m \log(z_m). \tag{5.1}$$

We are interested in the critical points of the multivalued function (5.1) on X. These points are algebraic functions of the parameters $s_1, s_2, \ldots, s_m$. Their number is the signed Euler characteristic $|\chi(X)|$, by [28]. In algebraic statistics, this is known as the *ML degree* of X.

Very affine varieties arising in physics are usually presented in the parametric form

$$X = \bigl\{x \in \mathbb{C}^n : f_1(x) \cdot f_2(x) \cdots f_m(x) \neq 0\bigr\},$$

where $f_1, f_2, \ldots, f_m$ are irreducible polynomials in n variables, and we set $z_i = f_i(x)$ in (5.1). Our task is to solve the following system of n equations in n unknowns:

$$\sum_{i=1}^{m} s_i f_i^{-1} \frac{\partial f_i}{\partial x_j} = 0 \quad \text{for } j = 1, 2, \ldots, n. \tag{5.2}$$

The left-hand side is a rational function. A tiny example with two solutions was seen in (2.3). As explained in [41], it is essential *not* to clear denominators. For our computations, we used the numerical software `HomotopyContinuation.jl` [13]. Systems with $|\chi| \leq 10000$ are easy to solve.

Experiment 5.1. The ML degree of $Y(3,7)$ is 3600. To verify this numerically, we set

$$M = \begin{bmatrix} 1 & 0 & 0 & 1 & 1 & 1 & 1 \\ 0 & 1 & 0 & 1 & x_1 & x_2 & x_3 \\ 0 & 0 & 1 & 1 & x_4 & x_5 & x_6 \end{bmatrix}. \tag{5.3}$$

Here, $n = 6$ and $m = 28 + 7 = 35$. The polynomials $f_i(x)$ come in two groups. First, there are 28 non-constant 3×3 minors of M. And, second, there are the seven conic conditions. This gives six equations (5.2) in six variables x_j that depend on 35 parameters s_i. It takes `HomotopyContinuation.jl` around 200 seconds to compute 3600 distinct complex solutions.

The main contribution of this section is the lower bound on the ML degree of $Y(3,8)$.

Experiment 5.2 (Proof and discussion for Theorem 4.1). The computation of the number 4884387 is the highlight of this section. This is analogous to Experiment 5.1, but it is now much harder. We will explain what was done. It starts with the parametrization

$$M' = \begin{bmatrix} 1 & 0 & 0 & 1 & 1 & 1 & 1 & 1 \\ 0 & 1 & 0 & 1 & x_1 & x_2 & x_3 & x_4 \\ 0 & 0 & 1 & 1 & x_5 & x_6 & x_7 & x_8 \end{bmatrix}.$$

The torus, in which the very affine variety $Y(3,8)$ lives, is defined by the complement of the vanishing of the polynomials f_i. These are given by the 48 non-constant 3×3-minors of M' and the 28 conditions that no six points lie on a conic. The resulting system consists of eight rational function equations in eight variables, and it depends on 76 parameters s_i.

We ran the software `HomotopyContiunation.jl` on this system of eight equations, using the method of monodromy loops, as explained in [41]. Our first serious experiment with this system ran 1708.32 hours on a `2x 12-Core Intel Xeon E5-2680 v3` at `2.5 GHz` with `512 GB RAM`. The computation needed over 74.55 GB. We obtained 4884318 distinct complex solutions. The problematic length of the computation is due to the sheer size. For each generated loop in the iteration, there are about 4 million that need to be tracked and checked against the existing list of solutions. We verified that the number achieved by our computations is in the correct order of magnitude using the estimation method of Hauenstein and Sherman [26].

At that point, we got in touch with Sascha Timme, who is the main developer of the software `HomotopyContinuation.jl`. Sascha kindly took over the computations, and he even used them to improve his implementation of the certification method in [12]. With this new implementation, he established a guarantee that there are 4884387 distinct non-singular solutions. The system is large and fairly ill-conditioned, so it is not surprising that it is missing 93 solutions compared to the number found in Olof Bergvall's forthcoming work. Sascha performed his computations with version 2.9.0 of `HomotopyContiunation.jl` on a `MacBook Pro` with the `M1 Pro Chip` and `32 GB of RAM`. The computations used all 10 threads. The total computation time was around 40 hours. The final count of 4884387 was already reached after running the monodromy loops for 16 hours. Just the certification of the solutions can now be performed in less than 30 minutes, using the new improvements for [12]. All the materials for these computations are made available at our `MathRepo` page.

To gain additional insight into the structures behind Theorem 4.1, we turned to tropical geometry. We applied the technique in [1, Section 8] to compute the tropical

critical points of the soft limit degeneration of the log-likelihood function. We discovered identifications as in [1, Table 4] of tropical critical points with stratification data.

To explain our findings, we start with the log-likelihood function for $n = 6$:

$$L = \sum_{1 \le i < j < k \le 6} s_{ijk} \cdot \log(p_{ijk}) + t \cdot \log(q). \tag{5.4}$$

The p_{ijk} are the 3×3 minors of the matrix M in (5.3), and q is the condition for the points to lie on a conic, shown explicitly in (1.1). The coefficients s_{ijk} and t in (5.4) are random real numbers. We know from Theorem 4.1 that L has 32 critical points $(x_1, x_2, x_3, x_4) \in \mathbb{C}^4$.

We now multiply some of the coefficients by a small positive parameter ε. The solutions depend on ε. Each coordinate $\hat{x}_i$ can be represented by a Puiseux series in ε, and ditto for the resulting quantities $\hat{p}_{ijk}$ and $\hat{q}$. The valuations of $(\hat{p}, \hat{q})$ are the *tropical critical points*.

A numerical method for computing tropical critical points and their multiplicities was presented in [1, Algorithm 1], along with an implementation using

`HomotopyContinuation.jl`.

We adapted this code to find tropical critical points on $Y(3, n)$ for $n = 6$ and $n = 7$.

Experiment 5.3 (Soft limits for $n = 6$). We multiply all coefficients s_{ij6} and t with ε. The zero vector is the unique tropical critical point of multiplicity $32 = 2 \cdot 16$, corresponding to the fibration $Y(3, 6) \to Y(3, 5)$. By contrast, suppose only t gets multiplied by ε. We obtain two tropical critical points, with multiplicities 26 and 6. The first group gives the solutions in $X(3, 6)$. The second group gives solutions in $\mathcal{M}_{0,6}$, with configurations on a conic.

Experiment 5.4 (Soft limits for $n = 7$). The 28 minors p_{ijk} have parameters s_{ijk}, and the seven conic conditions have parameters $t_{i_1,\ldots,i_6}$. All parameters having last index $k = i_6 = 7$ are multiplied by ε. This gives 46 tropical critical points. One of them has all coordinates zero. It has multiplicity $2880 = 90 \cdot 32$ and corresponds to the generic fiber of the map $Y(3, 7) \to Y(3, 6)$. The other 45 tropical critical points can be sorted into two classes of 15 and 30 each. Each of them has multiplicity 16. They correspond to the 45 ways of obtaining Eckardt points on a cubic surface. The resulting formula mirrors the structure of (4.1):

$$\chi(Y(3, 7)) = 3600 = 32 \cdot 90 + 45 \cdot 16.$$

This is the del Pezzo analog to the formula $\chi(X(3, 7)) = 1272 = 26 \cdot 42 + 15 \cdot 12$ for the stratified fibration $X(3, 7) \to X(3, 6)$. This formula was found in [21] and it was verified in [1, Table 4].

In a second experiment, we multiply the seven coefficients t for the conics by ε. We observe

$$\chi(Y(3,7)) = 3600 = 1272 + 7 \cdot 312 + 144.$$

The tropical multiplicities reveal the boundary of $Y(3,7)$ inside $X(3,7)$, as in (4.3).

In conclusion, the numerical computation of tropical critical points can yield considerable insight into the geometry of very affine varieties. Experiments 5.3 and 5.4 document this for del Pezzo moduli, and they suggest that tropical likelihood inference deserves further study.

6. Weyl groups, roots, and their ML degrees

The symmetric group acts on the configuration space $X(3,n)$ by permuting the n points. Our del Pezzo moduli spaces $Y(3,n)$ are more symmetric than that, because they admit an action of the Weyl group $W(E_n)$. We will make this very explicit for $n = 6, 7$.

The hyperplane arrangements of type E_6 and E_7 are defined by the linear forms seen from the matrix (1.3). Reflections at these hyperplanes generate the Weyl groups $W(E_6)$ and $W(E_7)$, which act on the key players in this paper. Their orders are 51840 and 2903040. By Remark 3.3, each group is generated by one Cremona involution in addition to the symmetric group that swaps labels. Using $d_1, \ldots, d_n$ for coordinates on $Y(3,n)$ following [34,36] and [35, Section 6], we express the Cremona involutions c_6 and c_7 as the following matrices:

$$c_6 = \frac{1}{3}\begin{bmatrix} 1 & 0 & -1 & 1 & 1 & -2 \\ 1 & 3 & 2 & 1 & 1 & 1 \\ -2 & 0 & -1 & -2 & -2 & -2 \\ 1 & 0 & -1 & 1 & -2 & 1 \\ 1 & 0 & -1 & -2 & 1 & 1 \\ -2 & 0 & -1 & 1 & 1 & 1 \end{bmatrix},$$

$$c_7 = \frac{1}{3}\begin{bmatrix} 1 & 0 & -1 & 1 & 1 & -2 & 0 \\ 1 & 3 & 2 & 1 & 1 & 1 & 0 \\ -2 & 0 & -1 & -2 & -2 & -2 & 0 \\ 1 & 0 & -1 & 1 & -2 & 1 & 0 \\ 1 & 0 & -1 & -2 & 1 & 1 & 0 \\ -2 & 0 & -1 & 1 & 1 & 1 & 0 \\ 1 & 0 & 2 & 1 & 1 & 1 & 3 \end{bmatrix}. \tag{6.1}$$

The matrix c_7 is obtained from the 7×7 matrix in equation (4-3) on [34, p. 337], namely, by the change of coordinates in equation (4-4) on [34, p. 338]. The matrix c_6 is obtained from c_7 by deleting the last row and last column.

The matrix in (1.3) gives a parametrization of $Y(3,6)$ and $Y(3,7)$, respectively. A natural idea is to explore the log-likelihood function (5.4) after plugging in this parametrization. For $n = 6$, the resulting function in d-coordinates equals

$$\sum_{1 \le i < j \le 6} s_{ij} \cdot \log(d_i - d_i) + \sum_{1 \le i < j < k \le 6} t_{ijk} \cdot \log(d_i + d_j + d_k) + v \cdot \log(d_1 + d_2 + d_3 + d_4 + d_5 + d_6). \tag{6.2}$$

If the coefficients s_{ij}, t_{ijk}, v are random real numbers, then this function has no critical points. We need to assume that these 36 coefficients sum to zero. Under that hypothesis, (6.2) is the logarithm of a rational function on the projective space $\mathbb{P}^5$, and the number of critical points is the Euler characteristic of the complement of the E_6 hyperplane arrangement in $\mathbb{P}^5$, which we denote by $\mathcal{A}(E_6)$. Similarly, we write $\mathcal{A}(E_7)$ for the complement of the 63 hyperplanes in $\mathbb{P}^6$. These complements are very affine varieties of dimension 5 and 6, respectively.

Proposition 6.1. *The ML degrees of $\mathcal{A}(E_6)$ and $\mathcal{A}(E_7)$ are equal to* 5040 *and* 368640.

Proof. The characteristic polynomials of the two hyperplane arrangements are

$$p_{E_6}(t) = (t-1)(t-4)(t-5)(t-7)(t-8)(t-11),$$
$$p_{E_7}(t) = (t-1)(t-5)(t-7)(t-9)(t-11)(t-13)(t-17).$$

The zeros of these polynomials are the *exponents* of the Coxeter groups $W(E_6)$ and $W(E_7)$. If we pass to affine space by declaring one of the hyperplanes to be at infinity, then the ML degree is the number of bounded regions in the arrangement. This number is computed by evaluating the reduced characteristic polynomial $p_{E_n}(t)/(t-1)$ at $t = 1$. In our two cases,

$$\begin{aligned} |\chi(\mathcal{A}(E_6))| &= 3 \cdot 4 \cdot 6 \cdot 7 \cdot 10 = 5040, \\ |\chi(\mathcal{A}(E_7))| &= 4 \cdot 6 \cdot 8 \cdot 10 \cdot 12 \cdot 16 = 368640. \end{aligned} \tag{6.3}$$

We verified both ML degrees by solving the likelihood equations, as in Section 5. ∎

We next examine the two morphisms of very affine varieties that are given by (1.3):

$$\mathcal{A}(E_6) \to Y(3,6) \quad \text{and} \quad \mathcal{A}(E_7) \to Y(3,7). \tag{6.4}$$

One might naively think that these maps are fibrations. But this is not the case. The fiber of the first map is the parabolic curve, which can be realized as the intersection of

the cubic surface with the quartic surface defined by its Hessian [23, Section 3]. This curve is generally smooth, but it is singular for special points in $Y(3,6)$. For instance, the parabolic curve of the Fermat cubic $x_0^3+x_1^3+x_2^3+x_3^3$ is reducible and it has 18 singular points, while for the Clebsch cubic $x_0^3+x_1^3+x_2^3+x_3^3-(x_0+x_1+x_2+x_3)^3$, it is irreducible with 10 singular points.

The failure of the maps in (6.4) to be fibrations explains the fact that the ML degrees in (6.3) are not divisible by those in Theorem 4.1. To reach the desired divisibility, we need additional linear constraints on the coefficients s_{ij}, t_{ijk}, v in (6.2). These constraints arise from representing our moduli spaces $Y(3,6)$ and $Y(3,7)$ in high-dimensional projective spaces. This goes back to Coble in 1928. We now review the relevant material from [23, 34, 35].

The *Yoshida variety* $\mathcal{Y}^\circ$ is the image of $\mathcal{A}(E_6)$ under the map $\mathbb{P}^5 \to \mathbb{P}^{39}$ that is given by the subroot systems of type $A_2^{\times 3}$. Its 40 coordinates are the 30 products $p_{125}p_{126}p_{134}p_{234}p_{356}p_{456}$ and the 10 products like $p_{123}p_{456}q$, up to relabeling, where p_{ijk} denotes 3×3 minors of (1.3). After dividing by $\prod_{1\le i<j\le 6}(d_i-d_j)$, each coordinate is a product of 9 roots of E_6. We write M_6 for the 36×40 incidence matrix where the rows are labeled by the roots and the columns are labeled by the Yoshida coordinates. This matrix has entries in $\{0,1\}$, with nine 1's in each column. By [35, Theorem 6.1], the rank of the matrix M_6 equals 16.

The *Göpel variety* $\mathcal{G}^\circ$ is the image of $\mathcal{A}(E_7)$ under the map $\mathbb{P}^5 \to \mathbb{P}^{134}$ that is given by the 135 subroot systems of type $A_1^{\times 7}$. Its coordinates are the 30 Fano configurations $p_{124}p_{235}p_{346}p_{457}p_{156}p_{267}p_{137}$ and the 105 Pascal configurations $p_{127}p_{347}p_{567}q$, up to relabeling. After dividing by $\prod_{1\le i<j\le 7}(d_i-d_j)$, each coordinate is a product of 7 roots of E_7. We write M_7 for the 63×135 incidence matrix where the rows are labeled by roots and the columns are labeled by Göpel coordinates. This matrix has entries in $\{0,1\}$, with seven 1's in each column. By [34, Theorem 6.1], the rank of the matrix M_7 equals 36. See [34, Theorem 6.2] for the homogeneous prime ideal in 135 variables that defines the Göpel variety.

Remark 6.2. The two varieties above are our moduli spaces: $\mathcal{Y}^\circ = Y(3,6)$ and $\mathcal{G}^\circ = Y(3,7)$. See [36, Lemma 3.1] for details on the tropical varieties corresponding to $\mathcal{A}(E_7)$, $\mathcal{A}(E_6)$, $\mathcal{Y}^\circ$, $\mathcal{G}^\circ$.

The virtue of the Yoshida and Göpel varieties is that our Weyl groups act by signed permutations on the coordinates of $\mathcal{Y}^\circ$ in $\mathbb{P}^{39}$ and of $\mathcal{G}^\circ$ in $\mathbb{P}^{134}$. These are simply the permutations of the subroot systems $A_2^{\times 3}$ in E_6 and $A_1^{\times 7}$ in E_7. Explicitly, we permute labels and apply the Cremona matrices in (6.1) to products of linear forms in d_1, d_2, d_3, d_4, d_5, d_6, d_7.

We now state the linear constraints on the 36, 63 coefficients s_{ij}, t_{ijk}, v in (6.2): these coefficient vectors must lie in the column space of the matrix M_6, M_7, respectively. This hypothesis ensures that (6.2) is well defined as a multivalued function on

$\mathcal{Y}^\circ = Y(3,6)$ and $\mathcal{G}^\circ = Y(3,7)$. Geometrically, we are considering the total spaces of the map $\mathcal{A}(E_6) \to \mathcal{Y}^\circ$ and $\mathcal{A}(E_7) \to \mathcal{G}^\circ$. We call these total spaces the *Yoshida parametrization* and the *Göpel parametrization*.

The numerical methods from Section 5 reveal the critical points of the log-likelihood function (6.2) where the coefficients are taken at random from these column spaces. The numbers of these critical points are the ML degrees of the parametrizations (6.4).

Experiment 6.3. The ML degree of the Yoshida parametrization equals $2880 = 90 \cdot 32$, and the ML degree of the Göpel parametrization equals $86400 = 24 \cdot 3600$.

The factor 24 is the size of the generic fiber of $\mathcal{A}(E_7) \to \mathcal{G}^\circ$. In other words, it is the number of cuspidal cubics through seven given points in $\mathbb{P}^2$; see [34, Section 4]. The number 90 in the first product is more mysterious to us. It should be the Euler characteristic of the parabolic curve [23] after the removal of a collection of special points.

7. Intermezzo from physics

Our point of departure is the *Koba–Nielsen string integral* [29], which we write as

$$\phi(s) = \varepsilon^{n-3} \int_{\mathcal{M}_{0,n}^+} \frac{1}{p_{12}p_{23}\cdots p_{n1}} \prod_{1 \le i < j \le n} p_{ij}^{\varepsilon \cdot s_{ij}}\, dp. \tag{7.1}$$

Here, $\mathcal{M}_{0,n}$ is the $(n-3)$-dimensional moduli space of n labeled points on the line $\mathbb{P}^1$. This is the quotient of the open Grassmannian $\mathrm{Gr}(2,n)^\circ$ modulo the torus action by $(\mathbb{C}^*)^n$. We write $p_{12}, p_{13}, \ldots, p_{n-1,n}$ for the Plücker coordinates on $\mathrm{Gr}(2,n)^\circ$. The positive Grassmannian $\mathrm{Gr}_+(2,n)$ consists of real points whose Plücker coordinates are positive. Its quotient modulo $(\mathbb{R}^+)^n$ is the *positive geometry* $\mathcal{M}_{0,n}^+$, to be identified with the orthant $\mathbb{R}^{n-3}_{>0}$. See [30, Section 3.5].

The physically meaningful quantities in (7.1) are the exponents s_{ij}. These are known as *Mandelstam invariants*. Using the *spinor-helicity formalism*, we write

$$s_{ij} = \det(K_i + K_j),$$

where $K_1, K_2, \ldots, K_n$ are 2×2 matrices of rank 1; i.e., we have points on the light-cone in $\mathbb{R}^{3,1}$. The K_i are momenta of n massless particles in a scattering process, so they sum to zero. The moduli space $\mathcal{M}_{0,n}^+$ is the *open string worldsheet* [2].

Momentum conservation $\sum_{i=1}^n K_i = 0$ translates into the relations $\sum_{i=1}^n s_{ij} = 0$ for all j, where $s_{jj} = 0$. These ensure that the integrand in (7.1) is well defined on $\mathcal{M}_{0,n}$. To evaluate the integral (7.1), one uses local coordinates $(0, z_2, z_3, \ldots, z_{n-2}, 1, \infty)$ so that $p_{ij} = -z_i + z_j$. We have $\mathcal{M}_{0,n}^+ \simeq \mathbb{R}^{n-3}_{>0}$ by assuming $0 < z_2 < \cdots < z_{n-2} < 1$.

While $\phi(s)$ is a transcendental function, its limit m_n for $\varepsilon \to 0$ is a rational function. Cachazo, He, and Yuan [20] computed it by summing over critical points of the scattering potential. For $n = 4$, this is the derivation from (2.3) to (2.6) in Section 2. For $n = 6$, we find

$$\begin{aligned} m_6 = {} & \frac{1}{s_{12}s_{34}s_{56}} + \frac{1}{s_{12}s_{56}s_{123}} + \frac{1}{s_{23}s_{56}s_{123}} + \frac{1}{s_{23}s_{56}s_{234}} + \frac{1}{s_{34}s_{56}s_{234}} \\ & + \frac{1}{s_{16}s_{23}s_{45}} + \frac{1}{s_{12}s_{34}s_{345}} + \frac{1}{s_{12}s_{45}s_{123}} + \frac{1}{s_{12}s_{45}s_{345}} + \frac{1}{s_{16}s_{23}s_{234}} \\ & + \frac{1}{s_{16}s_{34}s_{234}} + \frac{1}{s_{16}s_{34}s_{345}} + \frac{1}{s_{16}s_{45}s_{345}} + \frac{1}{s_{23}s_{45}s_{123}}. \end{aligned} \tag{7.2}$$

This is the *biadjoint scalar amplitude* [17,20]. Here, we abbreviate $s_{ijk} = s_{ij} + s_{ik} + s_{jk}$. The 14 summands in the amplitude (7.2) correspond to the planar trivalent trees with six labeled leaves, and hence to the vertices of the *associahedron* in $\mathbb{R}^3$. Summing the expressions (7.2) over all 60 cyclic orderings of the set $\{1, \ldots, 6\}$, one obtains the *cubic scalar amplitude*.

We now pass from $\mathcal{M}_{0,n}$ to the moduli space $X(3,n) = \mathrm{Gr}(3,n)^\circ/(\mathbb{C}^*)^n$ of n points in general position in $\mathbb{P}^2$. The Plücker coordinates on $\mathrm{Gr}(3,n)$ are denoted by p_{ijk}. We write $\mathfrak{s}_{ijk}$ for the Mandelstam invariants in CEGM theory [17]. In the physical setting, they are $\mathfrak{s}_{ijk} = \det(K_i + K_j + K_k)$, where $K_1, \ldots, K_n$ are 3×3 matrices of rank 1 whose sum has rank 1. As the analog to (7.1), Arkani-Hamed, He, and Lam [4, (6.11)] introduced the *stringy integral*

$$\psi(\mathfrak{s}) = \varepsilon^{2n-8} \int_{X_+(3,n)} \omega_{3,n} \prod_{1 \le i < j < k \le n} p_{ijk}^{\varepsilon \cdot \mathfrak{s}_{ijk}}. \tag{7.3}$$

In the integrand, we see the canonical form of $X(3,n)$, given in [4, (6.8)], as

$$\omega_{3,n} = \frac{d^{3\times n}C}{\mathrm{vol}\, SL(3) \times GL(1)^n} \frac{1}{p_{123}p_{234}\cdots p_{n12}}.$$

Here, $(p_{123}p_{234}\cdots p_{n12})^{-1}$ is the 3-Parke–Taylor factor. The limit $\varepsilon \to 0$ is a rational function in the unknowns $\mathfrak{s}$ of degree

$$8 - 2n = -\dim(X(3,n)).$$

This is called the *CEGM amplitude*. It was computed from the scattering potential on $X(3,n)$ by Cachazo, Early, Guevara, and Mizera in [17]. Note that the integrand (7.3) is a well-defined rational function on the configuration space $X_+(3,n)$ because matrix kinematics requires $\sum_{j,k=1}^n \mathfrak{s}_{ijk} = 0$ for all i.

The role of the tree space in (7.2) is played by the tropicalization of $X_+(3,n)$, a polyhedral space with very rich combinatorics. To see the connection with (7.2),

we now fix $n = 6$, and we multiply the integrand in (7.3) by a factor representing the conic condition q in (1.1). This replaces the Parke–Taylor factor by the following rational function in Plücker coordinates, which is found in [16, Section 6]:

$$\frac{1}{p_{123}p_{234}p_{345}p_{456}p_{156}p_{126}}\left[\frac{p_{123}p_{156}p_{246}p_{345}}{p_{126}p_{135}p_{234}p_{456}}-1\right]^{-1}=\frac{p_{135}}{p_{123}p_{345}p_{156}q}, \tag{7.4}$$

The CEGM amplitude in this paper is an integral over $Y(3,6)$ with the integrand (7.4). Thus, we replace the configuration space $X(3,6)$ by the del Pezzo moduli space $Y(3,6)$. The analog to (7.4) for $n = 7$ involves two conic factors. Here, the number two is the codimension of the stratum $b \simeq \mathcal{M}_{0,7}$ inside $Y(3,7)$, seen in the end of Section 4.

The resulting CEGM amplitudes are rational functions, to be computed in Section 9. They are highly symmetric, reflecting the Weyl group combinatorics in Section 6. As in [20], the computation rests on summing over the critical points of the scattering potential L, which is shown in (5.4). The relevant numerical algebraic geometry is explained in Section 5.

The integrand on the right-hand side (7.4) appeared prominently in the developments that led to the amplituhedron. We found it explicitly in the 2010 article [33], which was inspired "*by Witten's proposal that the $N^{k-2}MHV$ superamplitude should be the integral of an open string current algebra correlator over the space of degree $k-1$ curves in supertwistor space $\mathbb{P}^{3|4}$*". By Cauchy's residue theorem, the sum of the four residues in $p_{135}/(p_{123}p_{345}p_{156}q)$ is equal to zero. Nandan, Volovich, and Wen [33] rewrite this identity of residues as follows:

$$\{123\}+\{345\}+\{156\}=-\{q\}. \tag{7.5}$$

The right-hand side points to positive del Pezzo geometry. The left-hand side is the *BCFW triangulation* of the *amplituhedron* $\mathcal{A}_{6,1,4}$, which is the image of a linear map

$$\mathrm{Gr}_+(1,6)\to\mathrm{Gr}(1,5).$$

To be precise, $\mathcal{A}_{6,1,4}$ is a cyclic 4-polytope with 6 vertices, by the identification of cyclic polytopes with totally positive matrices. Our polytope has precisely two triangulations, each into three 4-simplices. The left-hand side of (7.5) is one of these triangulations.

In Section 2, we explained the positive geometry structure on the moduli space $Y(3,n)$ for $n = 5$, by identifying this very affine surface with $\mathcal{M}_{0,5}$. The resulting amplitude, shown in (2.6), is a smaller version of that in (7.2). A key role was played by the *u-equations* in (2.4). Such u-equations define very affine varieties known as binary geometries, seen recently in [5, 27] at the interface of particle physics and

geometric combinatorics. Given any simple d-polytope P with m facets, we introduce one variable u_i for each facet. The u-equations are

$$u_i + \prod_j u_j^{\beta_{ij}} = 1 \quad \text{for } i = 1, 2, \ldots, m, \tag{7.6}$$

where j runs over all facets of P that are disjoint from facet i and the β_{ij} are positive integers. If there exist β_{ij} such that the variety V defined by (7.6) has dimension d and admits a stratification that induces a combinatorial isomorphism to P, then V is a *binary geometry*. If this happens with $\beta_{ij} = 1$ for all i, j, then the u-equations are *perfect*. The existence of binary geometries is rare, as explained in [5], where this was connected to *cluster algebras*. He, Li, Raman, and Zhang [27] study the scenarios when P is a generalized permutohedron.

For $n = 5, 6$, the regions of a del Pezzo surface are perfect binary geometries because they are triangles, quadrilaterals, and pentagons; see Theorem 3.1. By [5, Section VII], this would no longer hold if m-gons with $m \geq 6$ appeared. In Sections 8 and 9, we introduce u-variables for the moduli spaces $Y(3, 6)$ and $Y(3, 7)$, and we argue that these define perfect binary geometries. It is important to note that our approach does *not* use cluster algebra structures on Grassmannians. For instance, the cluster algebra structure on $\mathrm{Gr}(3, 6)$ is built on the root system D_4, while $Y(3, 6)$ rests on the root system E_6. We are hopeful that the new perfect binary geometries from del Pezzo surfaces will lead to new discoveries in physics.

8. Combinatorics of Pezzotopes

We now turn to the real geometry of the very affine varieties $Y(3, 6)$ and $Y(3, 7)$. Our aim is to characterize the moduli spaces of del Pezzo surfaces over the real numbers. This involves combinatorics and representation theory, which is the main theme in this section, as well as geometry and commutative algebra, which will occupy us in Section 9. Here is a key result.

Theorem 8.1. *The* real *moduli space* $Y(3, 6)$ *has* 432 *connected components, all* $W(E_6)$ *equivalent. The closure of each component is homeomorphic as a cell-complex to a simple* 4*-polytope with f-vector* $(45, 90, 60, 15)$. *The real moduli space* $Y(3, 7)$ *has* 60480 *connected components, all* $W(E_7)$ *equivalent, the closure of each is homeomorphic as a cell-complex to a simple* 6*-dimensional homology ball with f-vector* $(579, 1737, 2000, 1105, 297, 34)$.

By an abuse of terminology, we use the term *pezzotope* for the connected components and the polytope (in the case of $Y(3, 6)$) in this theorem. In the E_7 case, we do not yet know a realization of the component as a convex polytope, but we expect it to

be. Further justification is provided in Theorem 9.4, where a computation in commutative algebra is used to show that the boundary of this region in $Y(3,7)$ is a homology sphere of dimension 5.

We now embark on our combinatorial journey to the E_6 pezzotope and the E_7 pezzotope. The proof of Theorem 8.1 will be concluded in Section 9. A key point is that the Weyl groups act transitively on the regions. This result is due to Sekiguchi and Yoshida [37–39]. Our exposition follows that given by Hacking, Keel, and Tevelev in [25, Section 8]. Our contributions include the f-vectors and the convex realization of the E_6 pezzotope. Also, the number 60480 of regions appears to be new: we did not find it in the sources listed above.

We describe the simplicial complexes that are dual to the boundaries of the pezzotopes. Let $\mathcal{G}(E_n)$ denote the respective edge graph, with 15 vertices for $n = 6$ and with 34 vertices for $n = 7$. Each sphere is a flag simplicial complex; i.e., its simplices are the cliques in the graph. To present the combinatorics of the pezzotopes, it suffices to give the graphs $\mathcal{G}(E_n)$.

We begin with $n = 6$. The 15 vertices of $\mathcal{G}(E_6)$ are denoted by $u_1, u_2, \ldots, u_{15}$. They are root subsystems that are described by the colorful Petersen graph in Figure 4a. Each vertex label ijk refers to the root $d_i + d_j + d_k$. The roots $d_i - d_j$ are denoted by pairs ij. The first ten vertices are root subsystems A_1. They correspond to the vertex labels:

$$\begin{array}{lllll} u_1 : 125, & u_2 : 126, & u_3 : 134, & u_4 : 136, & u_5 : 145, \\ u_6 : 234, & u_7 : 235, & u_8 : 246, & u_9 : 356, & u_{10} : 456. \end{array} \tag{8.1}$$

These variables correspond to the ten triangles formed by the arrangement of six lines shown in Figure 3a. This correspondence was given by Sekiguchi in [38, Figure III].

The other five vertices of $\mathcal{G}(E_6)$ are root subsystems $A_2^{\times 3}$, one for each color class of edges in Figure 4a. The three edges in a color class are the factors A_2, with three roots ij, ikl, jkl:

$$\begin{aligned} u_{11} &: \{\underline{12}, 134, 234, \underline{56}, 125, 126, \underline{34}, 356, 456\}, \\ u_{12} &: \{\underline{13}, 125, 235, \underline{46}, 134, 136, \underline{25}, 246, 456\}, \\ u_{13} &: \{\underline{14}, 126, 246, \underline{35}, 134, 145, \underline{26}, 235, 356\}, \\ u_{14} &: \{\underline{15}, 136, 356, \underline{24}, 125, 145, \underline{36}, 234, 246\}, \\ u_{15} &: \{\underline{16}, 145, 456, \underline{23}, 126, 136, \underline{45}, 234, 235\}. \end{aligned} \tag{8.2}$$

The 15 edges of the Petersen graph are partitioned into five triples. Each triple is pairwise disjoint in the graph, and its underlined labels are also disjoint. See [39, Figure 2].

The graph $\mathcal{G}(E_6)$ has 60 edges, which come in two groups, namely, 30 edges of type $\{A_1, A_1\}$ and 30 edges of type $\{A_1, A_2^{\times 3}\}$. Those of type $\{A_1, A_1\}$ are the

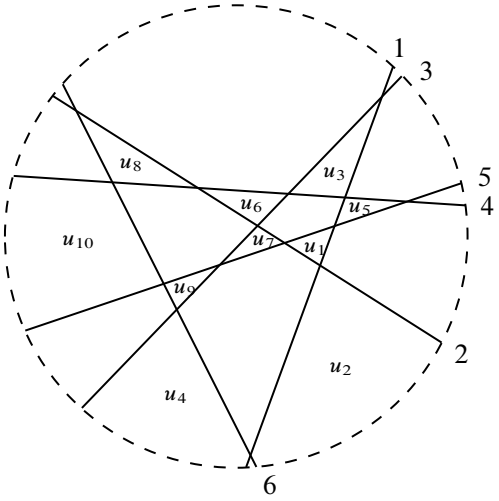

(a) The variables $u_1, u_2, \ldots, u_{10}$ for E_6 are the triangles in this line arrangement.

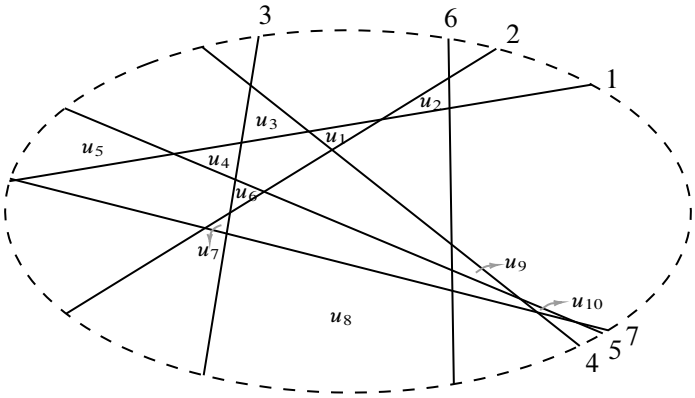

(b) These seven lines form 10 triangles corresponding to the 10 vertices of the tetradiagram in Figure 4b.

Figure 3. The triangles in these line arrangements are the vertex labels in Figure 4.

non-edges in the Petersen graph. For instance, $\{u_1, u_3\}$ is an edge of $\mathscr{G}(E_6)$ because $u_1 : 125$ and $u_3 : 134$ are not adjacent in the Petersen graph. The edges of type $\{A_1, A_2^{\times 3}\}$ arise from the $30 = 5 \cdot 3 \cdot 2$ inclusions of a root ijk in a system $A_2^{\times 3}$. For instance, $\{u_1, u_{14}\}$ is such an edge because $u_1 : 125$ is among the nine roots in u_{14}. We find that $\mathscr{G}(E_6)$ has 90 cliques of size three and 45 cliques of size four, and no larger cliques, which yields the first f-vector in Theorem 8.1.

We now offer two presentations of our pezzotope in the physics setting discussed in Section 7. The first is a variety as in (7.6). The second is an amplitude as in (7.2).

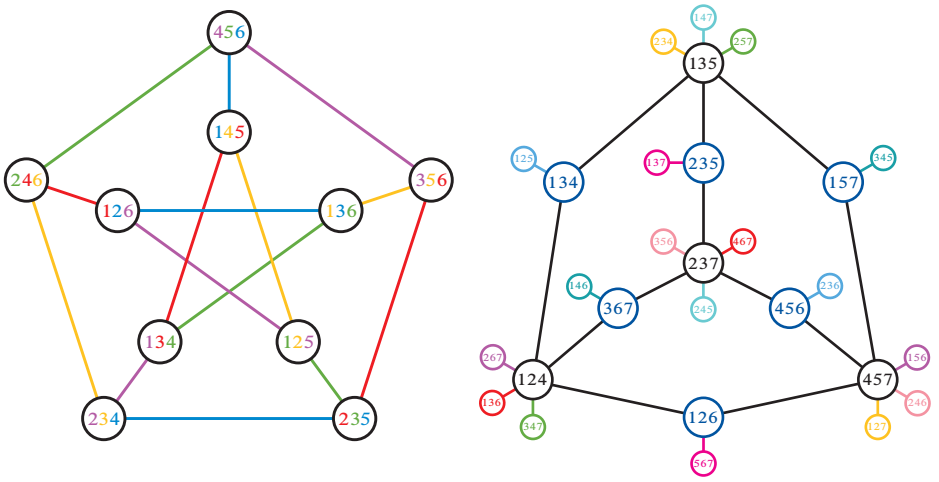

(a) (b)

Figure 4. Two graphs that reveal the combinatorics of the pezzotopes for $n = 6$ (left) and $n = 7$ (right). These diagrams are color-enhanced reproductions of those in [25, Figure 3].

Theorem 8.2. *The following u-equations define a perfect binary geometry (cf.* [5]*):*

$$\begin{aligned}
&u_1 + u_2u_5u_7u_{13}u_{15} \\
&= u_2 + u_1u_4u_8u_{12}u_{14} = u_3 + u_4u_5u_6u_{14}u_{15} \\
&= u_4 + u_2u_3u_9u_{11}u_{13} = u_5 + u_1u_3u_{10}u_{11}u_{12} \\
&= u_6 + u_3u_7u_8u_{12}u_{13} = u_7 + u_1u_6u_9u_{11}u_{14} \\
&= u_8 + u_2u_6u_{10}u_{11}u_{15} = u_9 + u_4u_7u_{10}u_{12}u_{15} \\
&= u_{10} + u_5u_8u_9u_{13}u_{14} = u_{11} + u_4u_5u_7u_8u_{12}u_{13}u_{14}u_{15} \\
&= u_{12} + u_2u_5u_6u_9u_{11}u_{13}u_{14}u_{15} = u_{13} + u_1u_4u_6u_{10}u_{11}u_{12}u_{14}u_{15} \\
&= u_{14} + u_2u_3u_7u_{10}u_{11}u_{12}u_{13}u_{15} = u_{15} + u_1u_3u_8u_9u_{11}u_{12}u_{13}u_{14} = 1. \quad (8.3)
\end{aligned}$$

The solution set in $\mathbb{R}^{15}_{\geq 0}$ *is combinatorially isomorphic to the* E_6 *pezzotope. The facets given by setting* $u_1, u_2, \ldots, u_{10}$ *to* 0 *are associahedra, and the facets for* $u_{11}, u_{12}, \ldots, u_{15}$ *are cubes. The* E_6 *amplitude* $\mathcal{A}_{E_6}$ *is the following sum over* 45 *terms, one for each vertex of the pezzotope:*

$$\begin{aligned}
&\frac{1}{s_1s_3s_8s_9} + \frac{1}{s_1s_3s_8s_{12}} + \frac{1}{s_1s_3s_9s_{11}} + \frac{1}{s_1s_3s_{10}s_{11}} + \frac{1}{s_1s_3s_{10}s_{12}} + \frac{1}{s_1s_4s_6s_{10}} \\
&\quad + \frac{1}{s_1s_4s_6s_{14}} + \frac{1}{s_1s_4s_8s_{12}} + \frac{1}{s_1s_4s_8s_{14}} + \frac{1}{s_1s_4s_{10}s_{12}} + \frac{1}{s_1s_6s_9s_{11}} + \frac{1}{s_1s_6s_9s_{14}}
\end{aligned}$$

$$
\begin{aligned}
&+\frac{1}{s_1s_6s_{10}s_{11}}+\frac{1}{s_1s_8s_9s_{14}}+\frac{1}{s_2s_3s_7s_{10}}+\frac{1}{s_2s_3s_7s_{13}}+\frac{1}{s_2s_3s_9s_{11}}+\frac{1}{s_2s_3s_9s_{13}}\\
&+\frac{1}{s_2s_3s_{10}s_{11}}+\frac{1}{s_2s_5s_6s_9}+\frac{1}{s_2s_5s_6s_{15}}+\frac{1}{s_2s_5s_7s_{13}}+\frac{1}{s_2s_5s_7s_{15}}+\frac{1}{s_2s_5s_9s_{13}}\\
&+\frac{1}{s_2s_6s_9s_{11}}+\frac{1}{s_2s_6s_{10}s_{11}}+\frac{1}{s_2s_6s_{10}s_{15}}+\frac{1}{s_2s_7s_{10}s_{15}}+\frac{1}{s_3s_7s_8s_{12}}\\
&+\frac{1}{s_3s_7s_8s_{13}}+\frac{1}{s_3s_7s_{10}s_{12}}+\frac{1}{s_3s_8s_9s_{13}}+\frac{1}{s_4s_5s_6s_{14}}+\frac{1}{s_4s_5s_6s_{15}}+\frac{1}{s_4s_5s_7s_8}\\
&+\frac{1}{s_4s_5s_7s_{15}}+\frac{1}{s_4s_5s_8s_{14}}+\frac{1}{s_4s_6s_{10}s_{15}}+\frac{1}{s_4s_7s_8s_{12}}+\frac{1}{s_4s_7s_{10}s_{12}}\\
&+\frac{1}{s_4s_7s_{10}s_{15}}+\frac{1}{s_5s_6s_9s_{14}}+\frac{1}{s_5s_7s_8s_{13}}+\frac{1}{s_5s_8s_9s_{13}}+\frac{1}{s_5s_8s_9s_{14}}.
\end{aligned}
\tag{8.4}
$$

The same data (u-equations and CEGM amplitude) for the E_7 pezzotope are displayed in Theorem 9.4. However, we do not yet know that they define a perfect binary geometry.

Proof. Each equation in (8.3) has a variable u_i and a monomial that is the product over all u_j not adjacent to u_i in the graph $\mathcal{G}(E_6)$. One checks computationally that the ideal generated by (8.3) is prime, and its variety in $\mathbb{C}^{15}$ has dimension 4 and degree 192. The variety in $\mathbb{R}^{15}_{\geq 0}$ admits a stratification that induces a combinatorial isomorphism to the pezzotope E_6. For example, the stratum obtained by restricting to $u_1 = 0$ is a curvy associahedron. Restricting further to $u_3 = 0$ reveals a curvy pentagonal face (cf. Section 2) of that associahedron.

We find the CEGM amplitude by summing (7.4) over all 32 critical points of (5.4):

$$
\sum_{c\in \mathrm{Crit}(L)}^{32} \frac{1}{\det(\Phi)}\left(\frac{p_{135}}{p_{123}p_{345}p_{561}q}\right)^2\Bigg|_c. \tag{8.5}
$$

Here, Φ is the toric Hessian of the scattering potential L, and the coefficients s_{ijk}, t in (5.4) are replaced by $s_1, s_2, \ldots, s_{15}$ using the rule in Remark 9.3. Then, (8.5) is a rational function in $s_1, s_2, \ldots, s_{15}$. We show by numerical evaluations that this rational function equals (8.4).

The derivation for $n = 7$ is analogous, using the data below. See Theorem 9.4. ∎

We now turn to $n = 7$. The graph $\mathcal{G}(E_7)$ has 34 vertices: ten of type A_1, twelve of type A_2, nine of type $A_3^{\times 2}$, and three of type A_7. The first ten are the labels in Figure 4b:

$$
\begin{aligned}
&u_1 : 124, \quad u_2 : 126, \quad u_3 : 134, \quad u_4 : 135, \quad u_5 : 157,\\
&u_6 : 235, \quad u_7 : 237, \quad u_8 : 367, \quad u_9 : 456, \quad u_{10} : 457.
\end{aligned}
\tag{8.6}
$$

The 12 vertices A_2 correspond to the pairs from (8.6) that are connected by an edge:

$$\begin{array}{lll} u_{11}:\{\underline{12},135,235\}, & u_{12}:\{\underline{14},157,457\}, & u_{13}:\{\underline{23},124,134\},\\ u_{14}:\{\underline{26},237,367\}, & u_{15}:\{\underline{37},135,157\}, & u_{16}:\{\underline{45},134,135\},\\ u_{17}:\{\underline{46},124,126\}, & u_{18}:\{\underline{57},235,237\}, & u_{19}:\{\underline{67},456,457\},\\ u_{20}:\{\underline{1},237,456\}, & u_{21}:\{\underline{3},126,457\}, & u_{22}:\{\underline{5},124,367\}. \end{array} \tag{8.7}$$

In the last row, $\underline{i}$ is the root $-d_i + \sum_{j=1}^{7} d_j$. Each subsystem $A_3^{\times 2}$ has 12 roots. These nine vertices of $\mathcal{G}(E_7)$ come in two types. The first six come from pairs of trivalent nodes:

$$\begin{aligned} u_{23}&:\{\underline{124},367,5,347,46,126,\underline{135},235,12,257,37,157\},\\ u_{24}&:\{\underline{124},134,23,136,46,126,\underline{237},235,57,467,1,456\},\\ u_{25}&:\{\underline{124},134,23,267,5,367,\underline{457},157,14,156,67,456\},\\ u_{26}&:\{\underline{135},157,37,147,45,134,\underline{237},456,1,245,26,367\},\\ u_{27}&:\{\underline{135},235,12,234,45,134,\underline{457},456,67,127,3,126\},\\ u_{28}&:\{\underline{237},235,57,356,26,367,\underline{457},157,14,246,3,126\}. \end{aligned} \tag{8.8}$$

We note that label 167 in [25, Figure 5] is incorrect. We corrected it to 156 in u_{25} above. The other three vertices of type $A_3^{\times 2}$ come from pairs of antipodal bivalent nodes:

$$\begin{aligned} u_{29}&:\{\underline{126},124,46,567,3,457,\underline{235},135,12,137,57,237\},\\ u_{30}&:\{\underline{134},124,23,125,45,135,\underline{456},237,1,236,67,457\},\\ u_{31}&:\{\underline{157},135,37,345,14,457,\underline{367},124,5,146,26,237\}. \end{aligned} \tag{8.9}$$

Finally, the graph $\mathcal{G}(E_7)$ has three vertices corresponding to root subsystems of type A_7:

$$\begin{aligned} u_{32}&:\{\underline{126},124,\underline{134},135,\underline{235},237,\underline{456},457,567,46,136,23,125,45,234,\\ &\qquad 12,137,57,467,1,236,67,127,3,13,56,2,47\},\\ u_{33}&:\{\underline{126},457,\underline{157},135,\underline{235},237,\underline{367},124,567,3,246,14,345,37,257,\\ &\qquad 12,137,57,356,26,146,5,347,46,35,24,7,16\},\\ u_{34}&:\{\underline{134},135,\underline{157},457,237,\underline{456},\underline{367},124,125,45,147,37,345,14,156,\\ &\qquad 67,236,1,245,26,146,5,267,23,15,36,4,27\}. \end{aligned} \tag{8.10}$$

The first eight roots in each A_7 form a cycle of length 8 in Figure 4b.

The graph $\mathcal{G}(E_7)$ has 297 edges, to be divided into several groups. There are 33 edges of type $\{A_1, A_1\}$, corresponding to non-edges in Figure 4b. The 24 edges of type $\{A_2, A_2\}$ arise from the inclusion of the pair of root systems in a common $A_3^{\times 2}$, but not in a common A_3. The edges $\{A_1, A_2\}$ come in two groups: 24 from the inclusion

of a root system ijk in A_2 and 60 from the pair not being contained in a common $A_3^{\times 2}$. There are 6 pairs of type $\{A_1, A_3^{\times 2}\}$ not contained in a common A_7 and such that any A_2 containing A_1 is disjoint from $A_3^{\times 2}$. Finally, we have five more groups of edges $\{A_1, A_3^{\times 2}\}$, $\{A_1, A_7\}$, $\{A_2, A_3^{\times 2}\}$, $\{A_2, A_7\}$, and $\{A_3^{\times 2}, A_7\}$, respectively, of size 54, 24, 36, 24, and 12, from the inclusion of the corresponding pairs. The clique complex of $\mathcal{G}(E_7)$ yields the second f-vector presented in Theorem 8.1.

9. Geometry of Pezzotopes

In Section 8, we offered a detailed combinatorial description of the two pezzotopes. We now return to the geometry of the moduli spaces they represent, starting with the algebraic expressions in Theorem 8.2. As always, our guiding principle is the trinity of real, complex, and tropical shapes in algebraic geometry. This section also harbors the proof of Theorem 8.1.

Theorem 8.2 gave an embedding of $Y(3,6)$ as a very affine variety in $(\mathbb{C}^*)^{15}$. The next result gives a parametric representation of our moduli space in that realization.

Proposition 9.1. *The variety of the u-equations in* (8.3) *has the parametrization*

$$u_1 = \frac{-q}{p_{126}p_{135}p_{234}p_{456}}, \quad u_2 = \frac{p_{134}p_{156}p_{235}p_{246}}{p_{135}p_{146}p_{234}p_{256}}, \quad u_3 = \frac{p_{134}p_{356}}{p_{135}p_{346}},$$
$$u_4 = \frac{p_{136}p_{145}}{p_{135}p_{146}}, \quad u_5 = \frac{p_{125}p_{136}p_{246}p_{345}}{p_{126}p_{135}p_{245}p_{346}}, \quad u_6 = \frac{p_{136}p_{235}}{p_{135}p_{236}},$$
$$u_7 = \frac{p_{123}p_{145}p_{246}p_{356}}{p_{124}p_{135}p_{236}p_{456}}, \quad u_8 = \frac{p_{125}p_{356}}{p_{135}p_{256}}, \quad u_9 = \frac{p_{125}p_{134}}{p_{124}p_{135}},$$
$$u_{10} = \frac{p_{145}p_{235}}{p_{135}p_{245}}, \quad u_{11} = \frac{p_{135}p_{234}}{p_{134}p_{235}}, \quad u_{12} = \frac{p_{135}p_{456}}{p_{145}p_{356}},$$
$$u_{13} = \frac{p_{124}p_{135}p_{256}p_{346}}{p_{125}p_{134}p_{246}p_{356}}, \quad u_{14} = \frac{p_{126}p_{135}}{p_{125}p_{136}}, \quad u_{15} = \frac{p_{135}p_{146}p_{236}p_{245}}{p_{136}p_{145}p_{235}p_{246}}.$$

Replacing the Plücker coordinates p_{ijk} with the 3×3 minors of (1.3)*, we obtain*

$$\begin{aligned}
u_1 &= (d_6 - d_3)(d_2 - d_5)(d_1 - d_4)(d_1 + d_2 + d_3 + d_4 + d_5 + d_6)/((d_4 + d_5 \\
&\quad + d_6)(d_2 + d_3 + d_4)(d_1 + d_3 + d_5)(d_1 + d_2 + d_6)), \\
u_2 &= (d_1 + d_3 + d_4)(d_1 + d_5 + d_6)(d_2 + d_3 + d_5)(d_2 + d_4 + d_6)/((d_2 + d_5 \\
&\quad + d_6)(d_2 + d_3 + d_4)(d_1 + d_4 + d_6)(d_1 + d_3 + d_5)), \\
u_3 &= (d_1 - d_4)(d_1 + d_3 + d_4)(d_5 - d_6)(d_3 + d_5 + d_6)/((d_4 - d_6)(d_3 + d_4 \\
&\quad + d_6)(d_1 - d_5)(d_1 + d_3 + d_5)), \\
u_4 &= (d_3 - d_6)(d_1 + d_3 + d_6)(d_4 - d_5)(d_1 + d_4 + d_5)/((d_4 - d_6)(d_1 + d_4 \\
&\quad + d_6)(d_3 - d_5)(d_1 + d_3 + d_5)),
\end{aligned}$$

$$
\begin{aligned}
u_5 &= (d_1+d_2+d_5)(d_1+d_3+d_6)(d_2+d_4+d_6)(d_3+d_4+d_5)/((d_3+d_4\\
&\quad +d_6)(d_2+d_4+d_5)(d_1+d_3+d_5)(d_1+d_2+d_6)),\\
u_6 &= (d_1-d_6)(d_1+d_3+d_6)(d_2-d_5)(d_2+d_3+d_5)/((d_2-d_6)(d_2+d_3\\
&\quad +d_6)(d_1-d_5)(d_1+d_3+d_5)),\\
u_7 &= (d_1+d_2+d_3)(d_1+d_4+d_5)(d_2+d_4+d_6)(d_3+d_5+d_6)/((d_4+d_5\\
&\quad +d_6)(d_2+d_3+d_6)(d_1+d_3+d_5)(d_1+d_2+d_4)),\\
u_8 &= (d_1-d_2)(d_1+d_2+d_5)(d_3-d_6)(d_3+d_5+d_6)/((d_2-d_6)(d_2+d_5\\
&\quad +d_6)(d_1-d_3)(d_1+d_3+d_5)),\\
u_9 &= (d_2-d_5)(d_1+d_2+d_5)(d_3-d_4)(d_1+d_3+d_4)/((d_3-d_5)(d_1+d_3\\
&\quad +d_5)(d_2-d_4)(d_1+d_2+d_4)),\\
u_{10} &= (d_1-d_4)(d_1+d_4+d_5)(d_2-d_3)(d_2+d_3+d_5)/((d_2-d_4)(d_2+d_4\\
&\quad +d_5)(d_1-d_3)(d_1+d_3+d_5)),\\
u_{11} &= (d_1-d_5)(d_1+d_3+d_5)(d_2-d_4)(d_2+d_3+d_4)/((d_2-d_5)(d_2+d_3\\
&\quad +d_5)(d_1-d_4)(d_1+d_3+d_4)),\\
u_{12} &= (d_1-d_3)(d_1+d_3+d_5)(d_4-d_6)(d_4+d_5+d_6)/((d_3-d_6)(d_3+d_5\\
&\quad +d_6)(d_1-d_4)(d_1+d_4+d_5)),\\
u_{13} &= (d_1+d_2+d_4)(d_1+d_3+d_5)(d_2+d_5+d_6)(d_3+d_4+d_6)/((d_3+d_5\\
&\quad +d_6)(d_2+d_4+d_6)(d_1+d_3+d_4)(d_1+d_2+d_5)),\\
u_{14} &= (d_2-d_6)(d_1+d_2+d_6)(d_3-d_5)(d_1+d_3+d_5)/((d_3-d_6)(d_1+d_3\\
&\quad +d_6)(d_2-d_5)(d_1+d_2+d_5)),\\
u_{15} &= (d_1+d_3+d_5)(d_1+d_4+d_6)(d_2+d_3+d_6)(d_2+d_4+d_5)/((d_2+d_4\\
&\quad +d_6)(d_2+d_3+d_5)(d_1+d_4+d_5)(d_1+d_3+d_6)).
\end{aligned}
$$

Proof. The proof is by computation. One checks that the above expressions for $u_1, \ldots, u_{15}$ satisfy the 15 equations in (8.3). Further, their Jacobian matrix has rank 4, so they parametrize an irreducible 4-dimensional variety in $(\mathbb{C}^*)^{15}$. This variety is $Y(3,6)$ by Theorem 8.2. ∎

Question 9.2. We wrote each u_i as a ratio of products of four roots of E_6. Such expressions were studied by Hacking, Keel, and Tevelev [25, Theorem 8.7], who called them D_4-*units*. They derive D_4-units also for E_7. How do we use their results for parametrizing the inclusion $Y(3,7) \subset (\mathbb{C}^*)^{34}$ given by the u-equations in (9.4) for the E_7 pezzotope?

We now turn to the CEGM amplitudes arising from del Pezzo moduli. For E_6, the expression as a rational function in $s_1, \ldots, s_{15}$ was displayed in (8.4). For E_7,

the formula is analogous but much larger, with 579 summands of degree -6 in 34 unknowns $s_1, \ldots, s_{34}$. Our readers may rapidly generate it with the `Macaulay2` code that is shown in Theorem 9.4.

The unknowns in (8.4) are the parameters in the log-likelihood function L on $Y(3,6)$. However, now, we use embedding of $Y(3,6)$ into $(\mathbb{C}^*)^{15}$ via the u-equations (8.3):

$$L = s_1 \cdot \log(u_1) + s_2 \cdot \log(u_2) + \cdots + s_{15} \cdot \log(u_{15}). \tag{9.1}$$

We are interested in the critical points of (9.1) on the variety defined by the 15 equations in (8.3). From a maximum likelihood perspective, we now face a constrained optimization problem. We already know (from Theorem 4.1) that this problem has 32 complex critical points, but it is very hard to find these using Lagrange multipliers in the unconstrained formulation. It is easier to compute the 32 critical points of (9.1) with the unconstrained formulation that is obtained from the parametrization in Proposition 9.1. That computation is equivalent to the one in local coordinates in (5.4) and also to the one via lifting to $\mathcal{A}(E_6)$ given in (6.2). We next present the transformation which makes these correspondences completely explicit.

Remark 9.3. If we substitute the Plücker parametrization from Proposition 9.1 into (9.1), then we obtain the expression for L in (5.4). Each Mandelstam invariant s_{ijk} is given as an integer linear combination of $s_1, \ldots, s_{15}$. Explicitly, we obtain the formulas

$$\begin{aligned} &s_{123} = s_7, s_{124} = -s_7 + s_9 + s_{13}, \\ &s_{125} = s_5 + s_8 + s_9 - s_{13} - s_{14}, \ldots, s_{456} = -s_1 - s_7 + s_{12}, t = s_1. \end{aligned}$$

These 21 linear forms in 15 unknowns $s_1, \ldots, s_6$ satisfy six independent linear constraints. These must be satisfied when using (5.4) in Plücker coordinates. For instance,

$$s_{125} + s_{135} + s_{145} + s_{156} + s_{235} + s_{245} + s_{256} + s_{345} + s_{356} + s_{456} + 2t = 0.$$

Similarly, if we substitute the D_4-units from Proposition 9.1 into (9.1), then we obtain the expression in (6.2), along with the linear constraints its coefficients s_{ij}, t_{ijk}, v must satisfy. Recall that these had been expressed by the matrix M_6 in Experiment 6.3. Everything in this remark extends directly to the case $n = 7$, but all expressions are larger.

We now complete the thread started at the beginning of the previous section.

Proof and discussion of Theorem 8.1. The relevant structures of the real moduli spaces were discovered by Sekiguchi and Yoshida [37–39]. They discussed the facets of the pezzotopes, but they did not give a list of faces. Also, Sekiguchi states the $n = 7$ result without proof. Their work was extended by Hacking, Keel, and Tevelev [25],

whose description we relied on in Section 8. We computed the number of connected components (432, resp., 60480) as the order of $W(E_n)$, modulo center, divided by the order of the automorphism group (S_5, resp., S_4) of the labeled diagrams in Figure 4. The fact that the Weyl group $W(E_n)$ acts transitively on the connected components of $Y(3,n)$ can be found in [39, Theorem 2] for $n = 6$ and in [37, Theorem 1] for $n = 7$.

We also derived the pezzotopes from data in [34, 35]. The Yoshida variety $\mathcal{Y}$ lives in $\mathbb{P}^{39}$, and the Göpel variety $\mathcal{G}$ lives in $\mathbb{P}^{134}$, namely, in the dense tori, by Remark 6.2. The Weyl groups act by permuting coordinates. Their tropicalizations were computed in [36, Lemma 3.1]. Namely, $\mathrm{trop}(\mathcal{Y})$ is a 4-dimensional fan with 76 rays and 1275 maximal cones, while $\mathrm{trop}(\mathcal{G})$ is a 6-dimensional fan with 1065 rays and 547155 maximal cones. The fibers of the surjection $\mathrm{trop}(\mathcal{G}) \to \mathrm{trop}(\mathcal{Y})$ are the tropical cubic surfaces that appear in [36, Section 5].

We explored the positive tropical varieties of $\mathcal{Y}$ and $\mathcal{G}$. Generators for their ideals are listed in [34, 35]. These furnish necessary conditions for membership in $\mathrm{trop}_+(\mathcal{Y})$ and $\mathrm{trop}_+(\mathcal{G})$ as follows: if a point w is in the positive tropical variety, then

$$\begin{aligned} &\forall \text{ generators } f = f_+ - f_- \text{ with } f_-, f_+ \in \mathbb{R}_{\geq 0}[x_1, \ldots, x_m]: \\ &\quad \mathrm{trop}(f_-)(w) = \mathrm{trop}(f_+)(w). \end{aligned} \tag{9.2}$$

We also know the tropical linear spaces $\mathrm{trop}(\mathcal{A}(E_6))$ and $\mathrm{trop}(\mathcal{A}(E_7))$, which map to $\mathrm{trop}(\mathcal{Y})$ and $\mathrm{trop}(\mathcal{G})$ via the horizontal maps in [36, (3.1)]. These are the linear maps given by the matrices $M_6 \in \{0,1\}^{36\times 40}$ and $M_7 \in \{0,1\}^{63\times 135}$ which we constructed in Section 6. For $n = 6, 7$, we computed the images of the rays of $\mathrm{trop}(\mathcal{A}(E_n))$ under the map M_n. Applying the criterion (9.2) to these images, we found 15 and 34 rays expected to live in $\mathrm{trop}_+(\mathcal{Y})$ and $\mathrm{trop}_+(\mathcal{G})$, respectively. To identify higher-dimensional cones, we applied the criterion to positive linear combinations of these rays. The f-vector of the output agrees with that stated in Theorem 8.1. These and further computational checks provide overwhelming evidence that the positive tropical varieties $\mathrm{trop}_+(\mathcal{Y})$ and $\mathrm{trop}_+(\mathcal{G})$ are simplicial fans which are dual to our pezzotopes.

Let us be even more explicit for $n = 6$. Our input is the data after [35, Theorem 6.1]. The fan $\mathrm{trop}(\mathcal{A}(E_6))$ has 36 rays of type A_1 and 120 rays of type A_2. The former map to 36 distinct rays in $\mathbb{N}^{40}$. The latter map to 40 distinct rays in $\mathbb{N}^{40}$. Each fiber in this 3-to-1 map corresponds to a color class in a Petersen graph like the one in Figure 4. For the membership criterion (9.2), we used the 270 four-term linear relations that cut out the 9-dimensional linear space in [35, Theorem 6.1]. The binomials are automatically satisfied because our 76 rays lie in the row space of M_6. Of the 36 rays of type A_1, ten passed the criterion. Of the 40 rays of type A_2, five passed. Up to the $W(E_6)$-action, these correspond to the root subsystems in (8.1) and (8.2). Among the $\binom{15}{2} = 105$ cones spanned by two rays, precisely 60 passed the necessary criterion to be contained in $\mathrm{trop}_+(\mathcal{Y})$, and similarly for triples and quadruples.

Two other methods for independent verification of Theorem 8.1 will be presented in Section 10. Their input is the familiar data for the *tropical Grassmannian* [31, Section 4.3]. They rely on modifications (Experiment 10.2) and chirotopes (Theorem 10.4).

It remains to show that our simplicial fans are normal fans of convex polytopes. This turned out to be more difficult than we had anticipated, and the issue is unresolved for $n = 7$. For $n = 6$, we obtained help from Moritz Firsching who found the following realization of the dual pezzotope:

$$\begin{bmatrix} 4 & -4 & 2 & 2 & -4 & -4 & 0 & 2 & -4 & 2 & -1 & 4 & -2 & 0 & -2 \\ 0 & -4 & -4 & 2 & 4 & 2 & -4 & 2 & 2 & -4 & -1 & -1 & 0 & 4 & 0 \\ 0 & 0 & 4 & -4 & 0 & -4 & 0 & 4 & 4 & -4 & 0 & 0 & 4 & 0 & -4 \\ 0 & 0 & 0 & 4 & 3 & -4 & 4 & 4 & -4 & 0 & -3 & 3 & 1 & 0 & 1 \end{bmatrix}. \tag{9.3}$$

One checks by direct computation that the convex hull of the 15 columns is a simplicial polytope with f-vector $(15, 60, 90, 45)$, and the 45 facets are precisely the 45 summands in (8.4); this polytope is *dual* to the E_6 pezzotope. We refer to Theorem 10.6 and Corollary 10.7 for the geometric realization of the E_6 pezzotope, as computed directly from a parametrization of one of the connected components of $Y(3, 6)$.

For $n = 7$, we need a 6×34 matrix with the analogous property, but we do not have it. We did verify that our simplicial complex on 34 vertices and 579 facets is a homology 5-sphere, so the term curvy 6-polytope is appropriate for its dual. Ideally, the polytopality of the pezzotopes should follow from general facts about positive tropical varieties, or from an argument about perfect binary geometries. But this is still missing. ∎

We now take a closer look at the E_7 pezzotope. The following result mirrors Theorem 8.2. However, the algebraic content is weaker. We believe that the u-equations below define a perfect binary geometry, but we currently have no proof. In particular, we conjecture that the 34 equations define a 6-dimensional subvariety of $(\mathbb{C}^*)^{34}$. This is an excellent challenge for the next generation in algebraic geometry software.

Theorem 9.4. *The E_7 pezzotope is characterized combinatorially by the 34 u-equations*

$$\begin{aligned} & u_1 + u_2u_{21}u_{22}u_{23}u_{24}u_{28}u_3u_{30}u_{32} \\ & = u_2 + u_1u_{19}u_{20}u_{25}u_{26}u_{27}u_{29}u_{31}u_{33}u_8 \\ & = u_3 + u_1u_{11}u_{13}u_{14}u_{16}u_{18}u_{25}u_{33}u_4u_6 = u_4 + u_{12}u_{17}u_{19}u_{21}u_{29}u_3u_5u_7u_8 \\ & = u_5 + u_{13}u_{20}u_{26}u_{28}u_{30}u_{31}u_{32}u_4u_6u_9 \\ & = u_6 + u_{10}u_{12}u_{14}u_{17}u_{19}u_{21}u_{22}u_{24}u_{25}u_{26}u_{27}u_{28}u_{29}u_3u_{34}u_5u_8 \end{aligned}$$

$$
\begin{aligned}
&= u_7 + u_{10}u_{14}u_{22}u_{24}u_{25}u_{26}u_{27}u_{28}u_{34}u_4\\
&= u_8 + u_{11}u_{13}u_{14}u_{16}u_{18}u_2u_{21}u_{22}u_{23}u_{24}u_{25}u_{28}u_{30}u_{32}u_{33}u_4u_6\\
&= u_9 + u_{11}u_{14}u_{16}u_{19}u_{21}u_{22}u_{23}u_{24}u_{25}u_{27}u_{29}u_{33}u_5\\
&= u_{10} + u_{15}u_{16}u_{23}u_{29}u_{30}u_{31}u_{33}u_6u_7\\
&= u_{11} + u_{15}u_{17}u_{22}u_{26}u_{27}u_{28}u_{29}u_3u_{30}u_{31}u_{34}u_8u_9\\
&= u_{12} + u_{14}u_{15}u_{16}u_{22}u_{23}u_{24}u_{25}u_{26}u_{27}u_{28}u_{29}u_{30}u_{31}u_{33}u_{34}u_4u_6\\
&= u_{13} + u_{14}u_{15}u_{16}u_{17}u_{19}u_{21}u_{22}u_{23}u_{24}u_{25}u_{26}u_{27}u_{28}u_{29}u_3u_{30}u_{31}u_{33}u_{34}u_5u_8\\
&= u_{14} + u_{12}u_{13}u_{17}u_{19}u_{20}u_{21}u_{26}u_{28}u_{29}u_3u_{30}u_{31}u_{32}u_6u_7u_8u_9\\
&= u_{15} + u_{10}u_{11}u_{12}u_{13}u_{19}u_{20}u_{21}u_{24}u_{25}u_{32}\\
&= u_{16} + u_{10}u_{12}u_{13}u_{17}u_{19}u_{20}u_{21}u_{22}u_{24}u_{25}u_{26}u_{27}u_{28}u_{29}u_3u_{30}u_{31}u_{32}u_{34}u_8u_9\\
&= u_{17} + u_{11}u_{13}u_{14}u_{16}u_{19}u_{20}u_{21}u_{22}u_{23}u_{24}u_{25}u_{26}u_{27}u_{28}u_{29}u_{30}u_{31}u_{32}u_{33}u_4u_6\\
&= u_{18} + u_{19}u_{20}u_{21}u_{22}u_{23}u_{24}u_{25}u_{26}u_{27}u_{28}u_{29}u_3u_{30}u_{31}u_{32}u_{33}u_8\\
&= u_{19} + u_{13}u_{14}u_{15}u_{16}u_{17}u_{18}u_2u_{22}u_{26}u_{28}u_{30}u_{31}u_{32}u_{34}u_4u_6u_9\\
&= u_{20} + u_{14}u_{15}u_{16}u_{17}u_{18}u_2u_{22}u_{34}u_5\\
&= u_{21} + u_1u_{13}u_{14}u_{15}u_{16}u_{17}u_{18}u_{22}u_{25}u_{26}u_{27}u_{28}u_{29}u_{30}u_{31}u_{33}u_{34}u_4u_6u_8u_9\\
&= u_{22} + u_1u_{11}u_{12}u_{13}u_{16}u_{17}u_{18}u_{19}u_{20}u_{21}u_{25}u_{26}u_{29}u_{30}u_{31}u_{32}u_{33}u_6u_7u_8u_9\\
&= u_{23} + u_1u_{10}u_{12}u_{13}u_{17}u_{18}u_{26}u_{34}u_8u_9\\
&= u_{24} + u_1u_{12}u_{13}u_{15}u_{16}u_{17}u_{18}u_{26}u_{29}u_{30}u_{31}u_{33}u_{34}u_6u_7u_8u_9\\
&= u_{25} + u_{12}u_{13}u_{15}u_{16}u_{17}u_{18}u_2u_{21}u_{22}u_{26}u_{28}u_{29}u_3u_{30}u_{31}u_{32}u_{34}u_6u_7u_8u_9\\
&= u_{26} + u_{11}u_{12}u_{13}u_{14}u_{16}u_{17}u_{18}u_{19}u_2u_{21}u_{22}u_{23}u_{24}u_{25}u_{29}u_{30}u_{32}u_{33}u_5u_6u_7\\
&= u_{27} + u_{11}u_{12}u_{13}u_{16}u_{17}u_{18}u_2u_{21}u_{30}u_{32}u_6u_7u_9\\
&= u_{28} + u_1u_{11}u_{12}u_{13}u_{14}u_{16}u_{17}u_{18}u_{19}u_{21}u_{25}u_{29}u_{33}u_5u_6u_7u_8\\
&= u_{29} + u_{10}u_{11}u_{12}u_{13}u_{14}u_{16}u_{17}u_{18}u_2u_{21}u_{22}u_{24}u_{25}u_{26}u_{28}u_{30}u_{32}u_{34}u_4u_6u_9\\
&= u_{30} + u_1u_{10}u_{11}u_{12}u_{13}u_{14}u_{16}u_{17}u_{18}u_{19}u_{21}u_{22}u_{24}u_{25}u_{26}u_{27}u_{29}u_{33}u_{34}u_5u_8\\
&= u_{31} + u_{10}u_{11}u_{12}u_{13}u_{14}u_{16}u_{17}u_{18}u_{19}u_2u_{21}u_{22}u_{24}u_{25}u_{32}u_{34}u_5\\
&= u_{32} + u_1u_{14}u_{15}u_{16}u_{17}u_{18}u_{19}u_{22}u_{25}u_{26}u_{27}u_{29}u_{31}u_{33}u_{34}u_5u_8\\
&= u_{33} + u_{10}u_{12}u_{13}u_{17}u_{18}u_2u_{21}u_{22}u_{24}u_{26}u_{28}u_3u_{30}u_{32}u_{34}u_8u_9\\
&= u_{34} + u_{11}u_{12}u_{13}u_{16}u_{19}u_{20}u_{21}u_{23}u_{24}u_{25}u_{29}u_{30}u_{31}u_{32}u_{33}u_6u_7 = 1. \qquad (9.4)
\end{aligned}
$$

The amplitude can be computed from the Stanley–Reisner ideal and its Alexander dual:

```
R = QQ[s1,s10,s11,s12,s13,s14,s15,s16,s17,s18,s19,s2,s20,s21,s22,s23,
s24,s25,s26,s27,s28,s29,s3,s30,s31,s32,s33,s34,s4,s5,s6,s7,s8,s9];
M = monomialIdeal(s1*s2,s1*s21,s1*s22,s1*s23,s1*s24,s1*s28,s1*s3,s1*s30,s1*s32,s10*s15,
s10*s16,s10*s23,s10*s29,s10*s30,s10*s31,s10*s33,s11*s15,s11*s17,s11*s22,s11*s26,
```

```
s11*s27,s11*s28,s11*s29,s11*s30,s11*s31,s11*s34,s12*s14,s12*s15,s12*s16,s12*s22,
s12*s23,s12*s24,s12*s25,s12*s26,s12*s27,s12*s28,s12*s29,s12*s30,s12*s31,s12*s33,
s12*s34,s13*s14,s13*s15,s13*s16,s13*s17,s13*s19,s13*s21,s13*s22,s13*s23,s13*s24,
s13*s25,s13*s26,s13*s27,s13*s28,s13*s29,s13*s30,s13*s31,s13*s33,s13*s34,s14*s17,
s14*s19,s14*s20,s14*s21,s14*s26,s14*s28,s14*s29,s14*s30,s14*s31,s14*s32,s15*s19,
s15*s20,s15*s21,s15*s24,s15*s25,s15*s32,s16*s17,s16*s19,s16*s20,s16*s21,s16*s22,
s16*s24,s16*s25,s16*s26,s16*s27,s16*s28,s16*s29,s16*s30,s16*s31,s16*s32,s16*s34,
s17*s19,s17*s20,s17*s21,s17*s22,s17*s23,s17*s24,s17*s25,s17*s26,s17*s27,s17*s28,
s17*s29,s17*s30,s17*s31,s17*s32,s17*s33,s18*s19,s18*s20,s18*s21,s18*s22,s18*s23,
s18*s24,s18*s25,s18*s26,s18*s27,s18*s28,s18*s29,s18*s30,s18*s31,s18*s32,s18*s33,
s19*s22,s19*s26,s19*s28,s19*s30,s19*s31,s19*s32,s19*s34,s2*s19,s2*s20,s2*s25,s2*s26,
s2*s27,s2*s29,s2*s31,s2*s33,s2*s8,s20*s22,s20*s34,s21*s22,s21*s25,s21*s26,s21*s27,
s21*s28,s21*s29,s21*s30,s21*s31,s21*s33,s21*s34,s22*s25,s22*s26,s22*s29,s22*s30,
s22*s31,s22*s32,s22*s33,s23*s26,s23*s34,s24*s26,s24*s29,s24*s30,s24*s31,s24*s33,
s24*s34,s25*s26,s25*s28,s25*s29,s25*s30,s25*s31,s25*s32,s25*s34,s26*s29,s26*s30,
s26*s32,s26*s33,s27*s30,s27*s32,s28*s29,s28*s33,s29*s30,s29*s32,s29*s34,s3*s11,
s3*s13,s3*s14,s3*s16,s3*s18,s3*s25,s3*s33,s3*s4,s3*s6,s30*s33,s30*s34,s31*s32,
s31*s34,s32*s33,s32*s34,s33*s34,s4*s12,s4*s17,s4*s19,s4*s21,s4*s29,s4*s5,s4*s7,
s4*s8,s5*s13,s5*s20,s5*s26,s5*s28,s5*s30,s5*s31,s5*s32,s5*s6,s5*s9,s6*s10,s6*s12,
s6*s14,s6*s17,s6*s19,s6*s21,s6*s22,s6*s24,s6*s25,s6*s26,s6*s27,s6*s28,s6*s29,s6*s34,
s6*s8,s7*s10,s7*s14,s7*s22,s7*s24,s7*s25,s7*s26,s7*s27,s7*s28,s7*s34,s8*s11,s8*s13,
s8*s14,s8*s16,s8*s18,s8*s21,s8*s22,s8*s23,s8*s24,s8*s25,s8*s28,s8*s30,s8*s32,s8*s33,
s9*s11,s9*s14,s9*s16,s9*s19,s9*s21,s9*s22,s9*s23,s9*s24,s9*s25,s9*s27,s9*s29,s9*s33);
dim M, degree M, betti mingens M
AmplitudeNumerator = sum first entries gens dual M
AmplitudeDenominator = product gens R
betti res dual M
```

The dual Betti sequence `579 1737 2000 1105 297 34 1` *verifies the Gorenstein property, so the simplicial complex dual to the* E_7 *pezzotope is indeed a homology sphere of dimension* 5.

Proof and discussion. We consider the graph $\mathcal{G}(E_7)$ whose 34 vertices were derived in (8.6), (8.7), (8.8), (8.9), and (8.10) from root subsystems in of E_7. Theorem 8.1 says that we also know the 297 edges of $\mathcal{G}(E_7)$. An explicit list is made using the techniques discussed in the proof.

In Theorem 9.4, we focus on the complementary set of $264 = \binom{34}{2} - 297$ non-edges of the graph $\mathcal{G}(E_7)$. Following (7.6), each u-equation has the form

$$u_i + \prod_j u_j^{\beta_{ij}} = 1,$$

where the product is over all indices j such that $\{i, j\}$ is a non-edge. We also know from Theorem 8.1 that the simplicial complex dual to the E_7 pezzotope is the clique complex of $\mathcal{G}(E_7)$. Therefore, the polynomial system (9.4) is a combinatorial encoding of both graph and E_7 pezzotope.

Now, we change variable names from u_i to $\mathtt{s}_i$, and we apply methods from combinatorial commutative algebra [32] to show that our pezzotope deserves to be called

a "curvy polytope". The ideal `M` is the Stanley–Reisner ideal of the clique complex: it is generated by 264 quadratic monomials, one for each of the non-edges. The commands `dim(M)` and `degree(M)` verify that the Stanley–Reisner ring has Krull dimension 6 and degree 579, which is the number of facets.

In the next line, the command `dual M` computes the ideal that is Alexander dual to `M`. See [32, Chapter 5] for a textbook introduction to Alexander duality. The command `betti res dual M` computes the minimal free resolution of the Alexander dual. We find that the resolution is linear, and the Betti numbers are the face numbers in Theorem 8.1. In fact, this output is precisely the minimal cellular resolution discussed in [32, Example 5.57]. By the Eagon–Reiner theorem [32, Theorem 5.56], we conclude that `M` is Cohen–Macaulay. The final Betti number `1` proves that `M` is a Gorenstein ideal, by [32, Theorem 5.61]. By Hochster's criterion, we conclude that our simplicial complex is a homology sphere of dimension 5. In conclusion, the E_7 pezzotope passes all homological tests for being a 6-dimensional polytope.

We now turn to the CEGM amplitude for $Y(3,7)$. We carried out the $n = 7$ computation analogous to (5.4), but now the sum is over the 3600 critical points found in Experiment 5.1. The computation is analogous to (8.5), but it is now much harder. The numerical output supports our conclusion that the structure agrees with that of the amplitudes in (7.2) and (8.4); namely, the CEGM amplitude for $Y(3,7)$ equals the sum of the reciprocals of 579 squarefree monomials of degree 6, one for each facet of the simplicial complex encoded by the ideal `M`. The Alexander dual ideal `dual M` is generated by 579 squarefree monomials of degree 28, namely, the complements of facets. We denote their sum by `AmplitudeNumerator`. We divide this numerator by `AmplitudeDenominator` $= \mathtt{s}_1\mathtt{s}_2\cdots\mathtt{s}_{34}$ to get the CEGM amplitude. ∎

Remark 9.5. From the u-equations in (9.4), we can read off all facets of the E_7 pezzotope. These 34 simple 5-polytopes come in five distinct combinatorial types, as follows.

- Three facets u_9, u_{11}, u_{27} are associahedra, with f-vector $(132, 330, 300, 120, 20)$.
- Twelve facets $u_6, u_8, u_{12}, u_{14}, u_{18}, u_{19}, u_{24}, u_{28}, u_{31}, u_{32}, u_{33}, u_{34}$ is the product of a 4-dimensional associahedron and a line segment, with f-vector $(84, 210, 196, 84, 16)$.
- Nine facets $u_{13}, u_{16}, u_{17}, u_{21}, u_{22}, u_{25}, u_{26}, u_{29}, u_{30}$ is the product of two pentagons and one line segment, with f-vector $(50, 125, 120, 55, 12)$.
- Six facets $u_2, u_3, u_5, u_7, u_{15}, u_{23}$ are polytopes with f-vector $(158, 395, 358, 142, 23)$.
- Four facets u_1, u_4, u_{10}, u_{20} are polytopes with f-vector $(168, 420, 380, 150, 24)$.

Thus, the first three types are products of associahedra, but the last two types are not.

10. Grassmannians, positive geometries, and beyond

In this final section, we return to the physics context of our work, namely, the axiomatic theory of positive geometries due to Arkani-Hamed, Bai, and Lam [3, 30], and the derivation of amplitudes from Grassmannians that was launched by Cachazo and collaborators [17, 20]. We saw first glimpses of this in Section 2, which described these structures for the surface $\mathcal{S}_4^\circ = \mathcal{M}_{0,5}$, and later in Section 7, which offered a guide to the relevant literature in physics.

In the end of Section 2, we gave a proof that the surface $\mathcal{S}_n^\circ$ is a positive geometry for $n = 4$. We start this section by extending that result to del Pezzo surfaces with $n \geq 5$.

Proposition 10.1. *The cubic surface $\mathcal{S}_6^\circ$ is a positive geometry for any of its* 130 *polygons. The degree four del Pezzo surface $\mathcal{S}_5^\circ$ is a positive geometry for any of its* 16 *pentagons.*

Proof. For every polygon P on $\mathcal{S}_6^\circ$, we can find six pairwise disjoint lines in $\mathcal{S}_6$ that are disjoint from the closure of P in $\mathcal{S}_6$. This can be checked combinatorially from the data in Example 3.2. Blowing down these six lines gives a birational map from $\mathcal{S}_6$ to $\mathbb{P}^2$ which is an isomorphism of semi-algebraic sets on the closure of the polygon P. In other words, we transform our curvy polygon P to a convex polygon P' in the real projective plane $\mathbb{P}^2$. Every convex polygon is a positive geometry [30, Section 1]. By [3, Section 4], the push-forward of the blow-up map transfers the positive geometry structure from $(\mathbb{P}^2, P')$ to $(\mathcal{S}_6, P)$.

The same argument works for the pentagons in $\mathcal{S}_5^\circ$. They are disjoint from five lines that can be blown down. We see this for the central pentagon in Figure 2. The argument does not work for the quadrilaterals on $\mathcal{S}_5^\circ$. This topic deserves further study. ∎

We now know that del Pezzo surfaces are positive geometries. Our goal is to establish the analogous result for their moduli spaces. This requires us to identify the canonical form, as in (2.5). This will be our focus later in the section. First, however, we turn to CEGM theory [16–19], which rests on the combinatorics of (tropical) Grassmannians. We will now explain how the pezzotopes are derived from first principles in this theory, directly from the Grassmannians $\mathrm{Gr}(3, n)$ for $n = 6, 7$. This extends the derivation of $\mathcal{M}_{0,5}$ from $\mathrm{Gr}(3, 5)$.

Fix $n = 6$ and consider $\mathrm{Gr}(3, 6)$ in its Plücker embedding in $\mathbb{P}^{19}$. The positive Grassmannian $\mathrm{Gr}_+(3, 6)$ consists of all points whose Plücker coordinates are positive. The tropical Grassmannian $\mathrm{Trop}(\mathrm{Gr}(3, 6))$, modulo lineality, is a 4-dimensional fan with 65 rays and 1005 maximal cones; see [40] and [31, Example 4.4.10 and Figure 5.4.1].

Experiment 10.2. The positive tropical Grassmannian $\mathrm{Trop}_+(\mathrm{Gr}(3,6))$ contains the following 14 vectors, here identified with variables in the E_6 amplitude (8.4):

$$\begin{aligned} s_2 &= \mathbf{e}_{156} & s_3 &= \mathbf{f}_{1234} & s_4 &= \mathbf{f}_{1236} & s_5 &= \mathbf{e}_{345} \\ s_6 &= \mathbf{f}_{2345} & s_7 &= \mathbf{e}_{123} & s_8 &= \mathbf{f}_{3456} & s_9 &= \mathbf{f}_{1256} \\ s_{10} &= \mathbf{f}_{1456} & s_{11} &= \mathbf{e}_{234} + \mathbf{e}_{156} & s_{12} &= \mathbf{e}_{123} + \mathbf{e}_{456} \\ s_{13} &= \mathbf{g}_{12,34,56} & s_{14} &= \mathbf{e}_{126} + \mathbf{e}_{345} & s_{15} &= \mathbf{g}_{16,45,23}. \end{aligned}$$

In the display above, $\mathbf{e}_{ijk}$ are unit vectors in $\mathbb{R}^{20}$, and we set

$$\mathbf{f}_{ijkl} = \mathbf{e}_{ijk} + \mathbf{e}_{ijl} + \mathbf{e}_{ikl} + \mathbf{e}_{jkl} \quad \text{and} \quad \mathbf{g}_{i_1i_2,i_3i_4,i_5i_6} = \mathbf{f}_{i_3i_4i_5i_6} + \mathbf{e}_{i_1i_5i_6} + \mathbf{e}_{i_2i_5i_6}.$$

Unfortunately, there is a typo in the indices for the vector $\mathbf{g}_{12,34,56}$ in [31, Example 4.4.10]. However, the indices in [40, Section 5] are correct.

We now describe an ab initio construction of the normal fan of our E_6 pezzotope that is motivated by physical considerations. The 15 rays in that fan are the 14 rays above, plus one additional ray s_1 that corresponds to the divisor

$$q = p_{123}p_{345}p_{156}p_{246} - p_{234}p_{456}p_{126}p_{135}.$$

The construction is based on the CEGM formula, which had revealed the E_6 amplitude to us in the first place. We work with the positive parametrization

$$M = \begin{bmatrix} 1 & 0 & 0 & ad & ad+ae+be & ad+ae+be+af+bf+cf \\ 0 & 1 & 0 & -d & -d-e & -d-e-f \\ 0 & 0 & 1 & 1 & 1 & 1 \end{bmatrix}. \tag{10.1}$$

This maps $\mathbb{R}^6_{>0}$ surjectively onto $X_+(3,6)$. From M, we compute the Newton polytope

$$P = \mathrm{Newt}\Big(\prod_{ijk} p_{ijk} \cdot q\Big).$$

This simple 4-polytope has $\mathrm{f} = (62, 124, 81, 19)$. We now form the *tropical scattering potential*

$$\mathcal{F}(y) = \sum_{ijk} \mathrm{trop}(p_{ijk})(y) \cdot \mathbf{e}_{ijk}.$$

Here, $\mathrm{trop}(p_{ijk})$ is the tropicalization of the Plücker coordinate p_{ijk} evaluated at M. For each of the 19 facet normals v_j of P, we obtain a positive tropical Plücker vector

$$\pi_j = \mathcal{F}(v_j).$$

These 19 rays include the 14 rays $s_2, s_3, \ldots, s_{15}$ above, while ray s_1 arises from the parameter t in the scattering potential L in (5.4). The 19 rays π_j are characterized as

follows. Sixteen of them are the rays of $\mathrm{Trop}_+(\mathrm{Gr}(3,6))$. The other three new rays are s_{11}, s_{12} and s_{14}. From this data, we define a rational function on the s-space $\mathbb{R}^{14}$,

$$\mathcal{A} = \sum_{\mathcal{C}\in N(P)} \prod_{\pi_j \in \mathrm{Rays}(\mathcal{C})} \frac{1}{\pi_j},$$

where π_j is now identified with a linear form in the s_i. The sum is over maximal cones $\mathcal{C}$ in the normal fan $N(P)$, and the product is over all rays in $\mathcal{C}$. Note that $N(P)$ is a simplicial fan. Next, by fixing various random integers for the Mandelstam invariants s_{ijk} and t, we evaluate the CEGM integral in (8.5) and its cyclic shift. Here, we sum over the 32 critical points:

$$\mathcal{A}_1 = \sum_{c\in \mathrm{Crit}(L)} \frac{1}{\det \Phi} \left(\frac{p_{135}}{p_{123}p_{345}p_{561}q} \right)^2 \Bigg|_c$$

and

$$\mathcal{A}_2 = \sum_{c\in \mathrm{Crit}(L)} \frac{1}{\det \Phi} \left(\frac{p_{246}}{p_{234}p_{456}p_{612}q} \right)^2 \Bigg|_c .$$

One can reconstruct 15 poles in each $\mathcal{A}_i$ from the (rational) values of these amplitudes. This is a difficult heuristic process, and it requires many evaluations, but we succeeded.

It remains to determine the dependence of $\mathcal{A}_1$ and $\mathcal{A}_2$ on the parameter t. For this, we evaluate the difference $\mathcal{A}_1 + \mathcal{A}_2 - \mathcal{A}$. This involves nine of the original 14 poles (together with t). These 9 poles are *exactly* the poles of the biadjoint scalar amplitude:

$$\mathcal{A}_1 + \mathcal{A}_2 - \mathcal{A} = m_6.$$

From this computation, we obtained the formula (8.4), and a representation of the pezzotope as a simplicial fan in $\mathbb{R}^{15}$, modulo lineality. One finally checks that the numerical value of the CEGM integral coincides with the value obtained combinatorially.

The difficulty in Experiment 10.2 arose from the fact that the positive Grassmannian is divided into pieces by the conic divisors. When applying the analogous methods to derive the E_7 pezzotope from $\mathrm{Gr}(3,7)$, this difficulty is magnified.

For that reason, in what follows we present a new approach, with a *different positive Grassmannian*, where that division of the positive part does not happen. Namely, we will switch signs of some of the Plücker coordinates of $\mathrm{Gr}(3,n)$ for $n = 6, 7$. After that sign change, we obtain a semi-algebraic set $\mathrm{Gr}_\chi(3,n)$ which now replaces $\mathrm{Gr}_+(3,n)$. The image of $\mathrm{Gr}_\chi(3,n)$ in the configuration space $X(3,n)$ is a connected component of $Y(3,n)$. The tropicalization of $\mathrm{Gr}_\chi(3,n)$ should be our fan $\mathrm{trop}_+(Y(3,n))$, after a modification for $n = 7$.

The letter χ stands for *chirotope*, which is one of the encodings of an *oriented matroid* [11]. In our context, χ is a function $\binom{[n]}{3} \to \{-1,+1\}$ that maps triples (i,j,k) to signs. Given any realizable chirotope χ, we substitute $p_{ijk} \mapsto \chi(i,j,k) \cdot p_{ijk}$, and we write $\mathrm{Gr}_\chi(3,n)$ for the positive Grassmannian after this sign change. The corresponding tropicalization is denoted by $\mathrm{trop}(\mathrm{Gr}_\chi(3,n))$. This was called the *chirotopal tropical Grassmannian* in [18, Section 13.1]. A point w lies in $\mathrm{trop}(\mathrm{Gr}_\chi(3,n))$ if and only if it satisfies condition (9.2) for *all* polynomials f in the Plücker ideal (after the sign change). This is the real version of the Fundamental Theorem of Tropical Geometry. We conjecture that, in our specific cases, it suffices to take f among the quadratic Plücker relations that generate the ideal of $\mathrm{Gr}(3,n)$.

Conjecture 10.3. *The Plücker quadrics are a positive tropical basis for* $\mathrm{Gr}_\chi(3,n)$.

In the discussion around (9.2), an analogous conjecture was tacitly made for the linear and binomial equations that generate the ideals of $\mathcal{Y}$ and $\mathcal{G}$. We now have the following theorem.

Theorem 10.4. *Suppose that Conjecture 10.3 is true, and the analogous statement holds for* $\mathcal{Y}$ *and* $\mathcal{G}$. *If* χ *is the chirotope for the arrangement of six lines in Figure 3a, then* $\mathrm{trop}(\mathrm{Gr}_\chi(3,6))$ *equals* $\mathrm{trop}_+(Y(3,6))$. *If* χ *is the chirotope for the seven lines in Figure 3b, then* $\mathrm{trop}(\mathrm{Gr}_\chi(3,7))$ *becomes* $\mathrm{trop}_+(Y(3,7))$ *after a modification that is explained below. Hence, our two pezzotopes can be read off from these two chirotopal tropical Grassmannians.*

Proof and discussion. The two line arrangements were presented by Sekiguchi and Yoshida in [39, Figure 4] and [38, (4)]. For both chirotopes χ, we computed the chirotopal tropical Grassmannians $\mathrm{trop}(\mathrm{Gr}_\chi(3,n))$ from the quadratic Plücker relations and we verified that it matches the data in Section 8. The correctness of this computation rests on Conjecture 10.3. This is analogous to what was assumed for the ideals of $\mathcal{Y}$ and $\mathcal{G}$ in the third paragraph in the proof of Theorem 8.1.

We now explain our computations, and how they imply Theorem 10.4. Let us start with $n = 6$. For each of the 65 rays of $\mathrm{trop}(\mathrm{Gr}(3,6))$, we tested whether it lies in the chirotopal positive Grassmannian. This is the case for precisely 15 rays, namely, the ten rays $\mathbf{e}_{ijk}$, where ijk appears in (8.1) and the five rays $\mathbf{g}_{12,56,34}$, $\mathbf{g}_{13,46,25}$, $\mathbf{g}_{14,35,26}$, $\mathbf{g}_{15,24,36}$, and $\mathbf{g}_{16,23,45}$ whose indices match (8.2). The subfan of $\mathrm{trop}(\mathrm{Gr}(3,6))$ induced on these 15 rays is combinatorially the normal fan of the E_6 pezzotope. Next, consider $n = 7$. The coarsest fan structure on $\mathrm{trop}(\mathrm{Gr}(3,7))$ has 616 rays, by [31, Theorem 5.4.1]. For each ray we used criterion (9.2) to test whether it lies in $\mathrm{trop}(\mathrm{Gr}_\chi(3,7))$. This is the case for precisely 31 rays. Among these are the ten rays $\mathbf{e}_{ijk}$, where ijk appears in the list (8.6). In order to match the induced subfan with the E_7 pezzotope, we had to add three additional rays: $\mathbf{e}_{126} + \mathbf{e}_{457}$, $\mathbf{e}_{124} + \mathbf{e}_{367}$

and $\mathbf{e}_{237} + \mathbf{e}_{456}$. Note that these six labels form a hexagon in Figure 4b. The bijection between the 34 rays we thus found and the set $\{u_1, u_2, \ldots, u_{34}\}$ appears on our `MathRepo` page.

To verify the matching, we check for each pair of rays whether its sum lies in $\mathrm{trop}(\mathrm{Gr}_\chi(3,7))$. This holds for 303 of the $\binom{34}{2} = 561$ pairs. Among these are all 297 edges of the graph $\mathcal{G}(E_7)$. The six extraneous pairs are `s1*s23`, `s2*s20`, `s10*s15`, `s13*s17`, `s21*s25`, `s26*s29`, here written in the `Macaulay2` notation from Theorem 9.4. We remove these six non-edges, and we check that all cliques of our graph $\mathcal{G}(E_7)$ do indeed give a cone in $\mathrm{trop}(\mathrm{Gr}_\chi(3,7))$.

The article [19] was essential for launching the current project. In fact, we first discovered the E_6 pezzotope by computing an CEGM amplitude as in [19]. For each realizable chirotope $\chi : \binom{[n]}{3} \to \{-1, +1\}$ with $n = 6, 7, 8$, Cachazo, Early, and Zhang determine an integrand $\mathcal{I}(\chi)$, which is a rational function in Plücker coordinates p_{ijk} of torus weight $(-3, \ldots, -3)$. These integrands satisfy non-trivial gluing conditions from flipping triangles in line arrangements. When the number of triangles in a line arrangement exceeds n, then the integrand has a non-trivial numerator, which must satisfy gluing conditions with its triangle flip neighbors. For $n = 6, 7, 8$, these gluing conditions are sufficient to uniquely determine the systems of integrands. The complexity of this process is high: there are 372, 27240, 4445640 reorientation classes of chirotopes for $n = 6, 7, 8$. The integrands relevant for us appear in [19, (3.26), (3.37)]. After relabeling to match the conventions in our Section 8, we have

$$\mathcal{I}(\chi_6) = \frac{q}{p_{125}p_{126}p_{134}p_{136}p_{145}p_{234}p_{235}p_{246}p_{356}p_{456}},$$
$$\mathcal{I}(\chi_7) = \frac{p_{123}p_{145}p_{357}}{p_{124}p_{126}p_{134}p_{135}p_{157}p_{235}p_{237}p_{367}p_{456}p_{457}},$$

where χ_6 and χ_7 are the chirotopes in Figure 3. The denominators are the ten triangles.

These two integrands are associated to $X(3,n)$, not to $Y(3,n)$. We compute their CEGM amplitudes by summing over critical points in $X(3,n)$, similar to (8.5):

$$m_n^{(3)}(\chi_n) = \sum_{c \in \mathrm{Crit}(L)} \frac{1}{\det(\Phi)} \mathcal{I}(\chi_n)^2|_c.$$

The number of summands is 26 for $n = 6$ and 1272 for $n = 7$. We find that $m_6^{(3)}(\chi_6)$ equals (8.4). However, there is a single linear relation among the 15 poles of $m_6^{(3)}(\chi_6)$:

$$\sum_{j=1}^{10} s_j = \sum_{j=11}^{15} s_j.$$

We note that, while the χ-region of $X(3,6)$ is unchanged when passing to $Y(3,6)$, the two compactifications are different. The story for $m_7^{(3)}(\chi_7)$ is similar: the connected component is unchanged when passing to $Y(3,7)$, but the compactification

is different. In this case, the amplitude has 31 poles and 441 nonzero 6-dimensional residues, one for each maximal cone in $\mathrm{Trop}(\mathrm{Gr}_{\chi_7}(3,7))$. From these, one derives the 579 summands of the CEGM amplitude. ∎

We now come to the punchline: *moduli of del Pezzo surfaces are positive geometries*. At present, we have a proof only for $n = 6$, but we conjecture the same for $n = 7$.

While the 432 connected components of $Y(3,6)$ are equivalent modulo the action of the Weyl group $W(E_6)$, we now single out one of them. This is denoted by $Y_+(3,6)$ and called the positive del Pezzo moduli space. Explicitly, it is the component of $Y(3,6)$ whose points are represented by a matrix as in (1.2), where all 3×3 minors and the conic condition are positive.

Theorem 10.5. *The moduli space $Y(3,6)$ is a positive geometry for any of its* 432 *regions, each of which is a curvy E_6 pezzotope.*

Proof. We prove that $(Y_+(3,6), \Omega)$ is a positive geometry. The canonical form is

$$\Omega = d\log\left(\frac{u_{10}}{u_5u_8u_9u_{13}u_{14}}\right) \wedge d\log\left(\frac{u_9u_{11}}{u_4u_7u_{12}u_{15}}\right) \\ \wedge d\log\left(\frac{u_4u_6u_{14}u_{15}}{u_3u_{13}}\right) \wedge d\log\left(\frac{u_1u_4u_8u_{12}u_{14}}{u_2}\right).$$

We applied the Weyl group action to this differential form. We found that it has precisely 432 distinct images. Hence, the symmetry group of the E_6 pezzotope acts on this form. The action is transitive on the set $\{u_1, \ldots, u_{10}\}$ of associahedral facets and on the set $\{u_{11}, \ldots, u_{15}\}$ of cubical facets. It hence suffices to compute the residue of Ω at one associahedron and at one cube, and to show that this residue matches the canonical form for these known positive geometries in dimension 3. The action by $W(E_6)$ is then used to conclude the proof.

We show that these residue of Ω are exactly the canonical forms of the 3-dimensional moduli spaces $\mathcal{M}_{0,6}$ and $\mathcal{M}_{0,4} \times \mathcal{M}_{0,4} \times \mathcal{M}_{0,4}$. The residue at $\{u_1 = 0\}$ equals

$$d\log\left(\frac{u_{10}}{u_8u_9u_{14}}\right) \wedge d\log\left(\frac{u_9u_{11}}{u_4u_{12}}\right) \wedge d\log\left(\frac{u_4u_6u_{14}}{u_3}\right). \tag{10.2}$$

This coincides with the canonical form of the worldsheet associahedron, after relabeling. The u-variables occurring in (10.2) satisfy the u-equations for $\mathcal{M}_{0,6}$, namely,

$$u_{10} + u_8u_9u_{14} = u_{11} + u_4u_8u_{12}u_{14} = u_6 + u_3u_8u_{12} \\ = u_9 + u_4u_{10}u_{12} = u_3u_{10}u_{11}u_{12} + u_{14} = u_8 + u_6u_{10}u_{11} \\ = u_4 + u_3u_9u_{11} = u_{12} + u_6u_9u_{11}u_{14} = u_3 + u_4u_6u_{14} = 1.$$

These nine equations arise from (8.3) by setting $u_1 = 0$. They give a perfect binary geometry on $\mathcal{M}^+_{0,6}$. On the other hand, the residue of Ω at the divisor $\{u_{11} = 0\}$ is the 3-form

$$d\log\left(\frac{u_{10}}{u_9}\right) \wedge d\log\left(\frac{u_6}{u_3}\right) \wedge d\log\left(\frac{u_1}{u_2}\right).$$

This is the canonical form of the curve 3-cube $\mathcal{M}^{\times 3}_{0,4}$. The equations in (8.3) simplify to

$$u_1 + u_2 = u_3 + u_6 = u_9 + u_{10} = 1.$$

We verified that $W(E_6)$ acts transitively on the 432 CEGM integrands (7.4), when evaluated on the d-matrix in (1.3), by relabeling with the Cremona map in (6.1). This completes the proof that $Y(3,6)$ is a positive geometry for any of its 432 regions.

To make sure, we also performed some checks in local coordinates on $Y(3,6)$. These verify that the form Ω is proportional to (7.4). For instance, consider the chart

$$M = \begin{bmatrix} 1 & 1 & 0 & 1 & 1 & 0 \\ x_1 & 0 & 1 & x_3 & 1 & 0 \\ x_2 & 0 & 0 & x_4 & 1 & 1 \end{bmatrix}.$$

All factors in (7.4) are non-constant. After simplifying the Jacobian matrix, we obtain the same expression by substituting 3×3 minors of M into Ω via Proposition 9.1:

$$\Omega = \frac{(x_2 - 1)d\,x_1 d\,x_2 d\,x_3 d\,x_4}{(x_1 - 1)x_2(x_4 - 1)(x_1x_2x_3 - x_1x_2x_4 - x_1x_3x_4 + x_2x_3x_4 + x_1x_4 - x_2x_3)}. \tag{10.3}$$

We are optimistic that a similar proof will work for $Y(3,7)$, using the facets in Remark 9.5. But we still lack the formula for Ω when $n = 7$. This is left for future work. ∎

We conclude by giving a parametrization for $Y_+(3,6)$, which encodes the compactification and E_6 amplitude in a very elegant way. From it, we realize the E_6 pezzotope as a polytope. This new realization is combinatorially equivalent to the dual of the polytope presented in (9.3). We define a birational map $\mathbb{R}^4 \dashrightarrow X(3,6)$ that restricts to a diffeomorphism $\mathbb{R}^4_{>0} \to Y_+(3,6)$. In the study of scattering amplitudes, it can be very helpful to construct such a parametrization, in the context of the CHY formula and string integrals. Such parameterizations are known and standard for $X(k,n)$; see, for example, [6, 15]. But finding one is generally difficult.

Theorem 10.6. *There is a birational map $\mathbb{R}^4 \dashrightarrow X(3,6)$ which restricts to a diffeomorphism $(\mathbb{R})^4_{>0} \to Y_+(3,6)$. Points in $Y_+(3,6)$ can be represented by the matrix*

$$\begin{bmatrix} 1 & 0 & 0 & 1 & \frac{y_2+1}{y_2} & \frac{y_2y_3+y_3+1}{y_2y_3} \\ 0 & 1 & 0 & -1 & -\frac{(y_1+1)(y_2+1)}{y_1y_2+y_2+1} & -\frac{(y_1+1)(y_2y_3+y_2y_4y_3+y_4y_3+y_3+y_2y_4+y_4+1)}{y_1y_2y_3+y_2y_3+y_1y_2y_4y_3+y_2y_4y_3+y_4y_3+y_3+y_1y_2y_4+y_2y_4+y_4+1} \\ 0 & 0 & 1 & 1 & 1 & 1 \end{bmatrix}.$$

Proof. We start from the canonical form of $Y_+(3,6)$ in the proof of Theorem 10.5:

$$\Omega = d\log\left(\frac{u_{10}}{u_5u_8u_9u_{13}u_{14}}\right) \wedge d\log\left(\frac{u_9u_{11}}{u_4u_7u_{12}u_{15}}\right) \wedge d\log\left(\frac{u_4u_6u_{14}u_{15}}{u_3u_{13}}\right) \wedge d\log\left(\frac{u_1u_4u_8u_{12}u_{14}}{u_2}\right).$$

Let y_i denote the rational functions appearing in the canonical form:

$$y_1 = \frac{u_{10}}{u_5u_8u_9u_{13}u_{14}}, \quad y_2 = \frac{u_9u_{11}}{u_4u_7u_{12}u_{15}},$$
$$y_3 = \frac{u_4u_6u_{14}u_{15}}{u_3u_{13}}, \quad y_4 = \frac{u_1u_4u_8u_{12}u_{14}}{u_2}.$$

We write the u-variables in terms of Plücker coordinates in Proposition 9.1 and evaluate them on the parameterization (10.1) of $X_+(3,6)$. The u-variables are now in terms of a, b, c, d, e, f. Modulo the torus action, we can fix $a = d = 1$. Rewriting b, c, e, f in terms of the y_i and substituting them into (10.1), we see that all 3×3 minors p_{ijk} and the conic condition q are positive for $y_j > 0$. This yields the desired birational map and its restriction. ∎

We collect all factors appearing in the evaluation of the u-variables on $M_{Y_+(3,6)}$:

$$\begin{aligned}
g_1 &= y_1 + 1, \quad g_2 = y_2 + 1, \quad g_3 = y_1y_2 + y_2 + 1, \quad g_4 = y_3 + 1,\\
g_5 &= y_2y_3 + y_3 + 1, \quad g_6 = y_4 + 1, \quad g_7 = y_1y_2y_4 + y_2y_4 + y_4 + 1,\\
g_8 &= y_2y_3 + y_2y_4y_3 + y_4y_3 + y_3 + y_2y_4 + y_4 + 1,\\
g_9 &= y_2y_3 + y_2y_4y_3 + y_4y_3 + y_3 + y_1y_2y_4 + y_2y_4 + y_4 + 1,\\
g_{10} &= y_2y_3 + y_1y_2y_4y_3 + y_2y_4y_3 + y_4y_3 + y_3 + y_1y_2y_4 + y_2y_4 + y_4 + 1,\\
g_{11} &= y_1y_2y_3 + y_2y_3 + y_1y_2y_4y_3 + y_2y_4y_3 + y_4y_3 + y_3 + y_1y_2y_4\\
&\quad + y_2y_4 + y_4 + 1.
\end{aligned}$$

These irreducible polynomials furnish a Minkowski sum decomposition of the E_6 pezzotope, in the sense that the face lattice of the Newton polytope of their product is isomorphic to the poset that is encoded by the u-equations. As an additional consistency check, we checked Corollary 10.7 using SageMath.

Corollary 10.7. *The Newton polytope P of the product $g_1g_2\cdots g_{11}$ is combinatorially equivalent to the dual polytope of equation* (9.3).

As in Experiment 10.2, we now form the tropical scattering potential for $Y_+(3,6)$:

$$\mathcal{F}_{Y_+(3,6)}(y) = \sum_{j=1}^{15} s_j \cdot \mathrm{trop}(u_j)(y).$$

Here, $\mathrm{trop}(u_j)$ is the tropicalization of u_j evaluated at the matrix $M_{Y_+(3,6)}(y)$. The tropical u-variables are nonnegative for all y. This ensures the convergence of the integral in (10.4) whenever the s_i are positive.

Theorem 10.8. *The tropical potential $\mathcal{F}_{Y_+(3,6)}(y)$ provides a bijection between the (inner) normal fan of the Newton polytope P defined in the previous corollary and the positive tropical del Pezzo moduli space* $\mathrm{Trop}_+(Y(3,6))$. *We can compute the E_6 amplitude through the global Schwinger parameterization* [18]*:*

$$\mathcal{A}_{E_6} = \int_{\mathbb{R}^4} \exp\bigl(-\mathcal{F}_{Y_+(3,6)}(y)\bigr) d\ y. \tag{10.4}$$

Proof. The proof follows the logic of Experiment 10.2. The facet normals of P are

$$\begin{aligned} &e_4,\ -e_4,\ -e_3,\ -e_2+e_3+e_4,\ -e_1, e_3, -e_2,\ e_4-e_1,\\ &e_2-e_1,\ e_1,\ e_2,\ e_4-e_2,\ -e_1-e_3,\ -e_1+e_3+e_4, e_3-e_2. \end{aligned}$$

We denote these vectors by $v_1,\ldots,v_{15}\in\mathbb{R}^4$. They are dual to the rays of $\mathrm{Trop}_+ Y(3,6)$ and yield the poles of the E_6 amplitude, as they satisfy

$$\mathrm{trop}(u_i)(v_j) = \delta_{i,j}$$

and $\mathcal{F}_{Y_+(3,6)}(v_j) = s_j$. Moreover, the general rule for Newton polytope decompositions holds here: $\mathcal{F}_{Y_+(3,6)}(y)$ is linear on exactly the cones in the inner normal fan of P. As in [18], it follows that (10.4) is the sum of the Laplace transforms of the inner normal cones to the 45 vertices of P, and so,

$$\int_{\mathbb{R}^4} \exp\bigl(-\mathcal{F}_{Y_+(3,6)}(y)\bigr) d\ y = \sum_{\mathcal{C}\in N(P)} \int_{(\mathbb{R}_{>0})^4} \exp\left(-\sum_{j=1}^{4} t_{i_j} s_{i_j}\right) d\ t.$$

The inner sum in the exponential is over the four rays s_{i_1}, s_{i_2}, s_{i_3}, s_{i_4} of the cone $\mathcal{C}$. The outer sum on the right-hand side equals the E_6 amplitude $\mathcal{A}_{E_6}$ in Theorem 8.2. ∎

Acknowledgments. The authors are very grateful to seven colleagues for help with this project. Tobias Boege contributed software for Section 3. Moritz Firsching discovered the E_6 polytope in (9.3), and Sascha Timme found the ML degree of $Y(3,8)$ with `HomotopyContinuation.jl`. Nima Arkani-Hamed offered guidance on binary geometries, and Freddy Cachazo helped them with integrands including (10.3). Thomas Endler created the diagrams in Figures 2 and 4. They thank Olof Bergvall for references for Theorem 4.1 and for useful conversations. Finally, they thank the referees for their comments.

References

[1] D. Agostini, T. Brysiewicz, C. Fevola, L. Kühne, B. Sturmfels, and S. Telen, Likelihood degenerations. *Adv. Math.* **414** (2023), article no. 108863 Zbl 1535.14106 MR 4539061

[2] N. Arkani-Hamed, Y. Bai, S. He, and G. Yan, Scattering forms and the positive geometry of kinematics, color and the worldsheet. *J. High Energy Phys.* (2018), no. 5, article no. 096 Zbl 1391.81200 MR 3832668

[3] N. Arkani-Hamed, Y. Bai, and T. Lam, Positive geometries and canonical forms. *J. High Energy Phys.* (2017), no. 11, article no. 039 Zbl 1383.81273 MR 3747267

[4] N. Arkani-Hamed, S. He, and T. Lam, Stringy canonical forms. *J. High Energy Phys.* (2021), no. 2, article no. 069 Zbl 1460.83083 MR 4260349

[5] N. Arkani-Hamed, S. He, T. Lam, and H. Thomas, Binary geometries, generalized particles and strings, and cluster algebras. *Phys. Rev. D* **107** (2023), no. 6, article no. 066015 MR 4576219

[6] N. Arkani-Hamed, T. Lam, and M. Spradlin, Positive configuration space. *Comm. Math. Phys.* **384** (2021), no. 2, 909–954 Zbl 1471.14101 MR 4259378

[7] O. Bergvall, Equivariant cohomology of the moduli space of genus three curves with symplectic level two structure via point counts. *Eur. J. Math.* **6** (2020), no. 2, 262–320 Zbl 1440.14145 MR 4098091

[8] O. Bergvall and F. Gounelas, Cohomology of moduli spaces of Del Pezzo surfaces. *Math. Nachr.* **296** (2023), no. 1, 80–101 Zbl 1535.14084 MR 4553589

[9] A. Betten and F. Karaoglu, The Eckardt point configuration of cubic surfaces revisited. *Des. Codes Cryptogr.* **90** (2022), no. 9, 2159–2180 Zbl 1496.05015 MR 4473955

[10] T. Bitoun, C. Bogner, R. P. Klausen, and E. Panzer, Feynman integral relations from parametric annihilators. *Lett. Math. Phys.* **109** (2019), no. 3, 497–564 Zbl 1412.81141 MR 3910134

[11] A. Björner, M. Las Vergnas, B. Sturmfels, N. White, and G. M. Ziegler, *Oriented matroids*. Encyclopedia Math. Appl. 46, Cambridge University Press, Cambridge, 1993 Zbl 0773.52001 MR 1226888

[12] P. Breiding, K. Rose, and S. Timme, Certifying zeros of polynomial systems using interval arithmetic. *ACM Trans. Math. Software* **49** (2023), no. 1, article no. 11 Zbl 07908573 MR 4567897

[13] P. Breiding and S. Timme, HomotopyContinuation.jl: A package for homotopy continuation in Julia. In *Math. software – icms 2018*, pp. 458–465, Springer, 2018 Zbl 1396.14003

[14] F. C. S. Brown, Multiple zeta values and periods of moduli spaces $\overline{\mathfrak{M}}_{0,n}$. *Ann. Sci. Éc. Norm. Supér. (4)* **42** (2009), no. 3, 371–489 Zbl 1216.11079 MR 2543329

[15] F. Cachazo and N. Early, Planar kinematics: Cyclic fixed points, mirror superpotential, k-dimensional Catalan numbers, and root polytopes. *Ann. Inst. Henri Poincaré Comb. Phys. Interact.* (2024), DOI 10.4171/AIHPD/185

[16] F. Cachazo and N. Early, Biadjoint scalars and associahedra from residues of generalized amplitudes. *J. High Energy Phys.* (2023), no. 10, article no. 15 Zbl 07774620 MR 4651040

[17] F. Cachazo, N. Early, A. Guevara, and S. Mizera, Scattering equations: From projective spaces to tropical Grassmannians. *J. High Energy Phys.* (2019), no. 6, article no. 39 Zbl 1445.81064 MR 3982543

[18] F. Cachazo, N. Early, and Y. Zhang, Color-dressed generalized biadjoint scalar amplitudes: Local planarity. *SIGMA Symmetry Integrability Geom. Methods Appl.* **20** (2024), article no. 016 Zbl 1545.14059 MR 4706977

[19] F. Cachazo, N. Early, and Y. Zhang, Generalized color orderings: CEGM integrands and decoupling identities. *Nuclear Phys. B* **1004** (2024), article no. 116552 Zbl 07866023 MR 4741472

[20] F. Cachazo, S. He, and Y. Yuan, Scattering of massless particles: Scalars, gluons and gravitons. *J. High Energy Phys.* (2014), article no. 33 Zbl 1391.81198

[21] F. Cachazo, B. Umbert, and Y. Zhang, Singular solutions in soft limits. *J. High Energy Phys.* (2020), no. 5, article no. 148 MR 4112295

[22] F. Catanese, S. Hoşten, A. Khetan, and B. Sturmfels, The maximum likelihood degree. *Amer. J. Math.* **128** (2006), no. 3, 671–697 Zbl 1123.13019 MR 2230921

[23] E. Colombo, B. van Geemen, and E. Looijenga, Del Pezzo moduli via root systems. In *Algebra, arithmetic, and geometry: in honor of Yu. I. Manin. Vol. I*, pp. 291–337, Progr. Math. 269, Birkhäuser, Boston, MA, 2009 Zbl 1195.14051 MR 2641175

[24] S. L. Devadoss, Combinatorial equivalence of real moduli spaces. *Notices Amer. Math. Soc.* **51** (2004), no. 6, 620–628 Zbl 1093.14509 MR 2064149

[25] P. Hacking, S. Keel, and J. Tevelev, Stable pair, tropical, and log canonical compactifications of moduli spaces of del Pezzo surfaces. *Invent. Math.* **178** (2009), no. 1, 173–227 Zbl 1205.14012 MR 2534095

[26] J. Hauenstein and S. Sherman, Using monodromy to statistically estimate the number of solutions. In *2nd IMA Conference on Mathematics of Robotics*, pp. 37–46, Springer Proc. Adv. Robot. 21, 2022 Zbl 07608753

[27] S. He, Z. Li, P. Raman, and C. Zhang, Stringy canonical forms and binary geometries from associahedra, cyclohedra and generalized permutohedra. *J. High Energy Phys.* (2020), no. 10, article no. 054 Zbl 1456.83101 MR 4204051

[28] J. Huh, The maximum likelihood degree of a very affine variety. *Compos. Math.* **149** (2013), no. 8, 1245–1266 Zbl 1282.14007 MR 3103064

[29] Z. Koba and H. Nielsen, Manifestly crossing invariant parametrization of n meson amplitude. *Nucl. Phys. B* **12** (1969), 517–536

[30] T. Lam, An invitation to positive geometries. In *Open problems in algebraic combinatorics*, pp. 159–179, Proc. Sympos. Pure Math. 110, American Mathematical Society, Providence, RI, 2024 MR 4780729

[31] D. Maclagan and B. Sturmfels, *Introduction to tropical geometry*. Grad. Stud. Math. 161, American Mathematical Society, Providence, RI, 2015 Zbl 1321.14048 MR 3287221

[32] E. Miller and B. Sturmfels, *Combinatorial commutative algebra*. Grad. Texts in Math. 227, Springer, New York, 2005 Zbl 1090.13001 MR 2110098

[33] D. Nandan, A. Volovich, and C. Wen, A Grassmannian étude in NMHV minors. *J. High Energy Phys.* (2010), no. 7, article no. 061 Zbl 1290.81075 MR 2719982

[34] Q. Ren, S. V. Sam, G. Schrader, and B. Sturmfels, The universal Kummer threefold. *Exp. Math.* **22** (2013), no. 3, 327–362 Zbl 1312.14103 MR 3171096

[35] Q. Ren, S. V. Sam, and B. Sturmfels, Tropicalization of classical moduli spaces. *Math. Comput. Sci.* **8** (2014), no. 2, 119–145 Zbl 1305.14031 MR 3224624

[36] Q. Ren, K. Shaw, and B. Sturmfels, Tropicalization of del Pezzo surfaces. *Adv. Math.* **300** (2016), 156–189 Zbl 1375.14218 MR 3534831

[37] J. Sekiguchi, Geometry of 7 lines on the real projective plane and the root system of type E_7. *Sūrikaisekikenkyūsho Kōkyūroku* (1997), no. 986, 1–8 Zbl 0925.14028 MR 1604057

[38] J. Sekiguchi, Configurations of seven lines on the real projective plane and the root system of type E_7. *J. Math. Soc. Japan* **51** (1999), no. 4, 987–1013 Zbl 0948.52010 MR 1705257

[39] J. Sekiguchi and M. Yoshida, $W(E_6)$-action on the configuration space of six lines on the real projective plane. *Kyushu J. Math.* **51** (1997), no. 2, 297–354 Zbl 0932.14027 MR 1470158

[40] D. Speyer and B. Sturmfels, The tropical Grassmannian. *Adv. Geom.* **4** (2004), no. 3, 389–411 Zbl 1065.14071 MR 2071813

[41] B. Sturmfels and S. Telen, Likelihood equations and scattering amplitudes. *Algebr. Stat.* **12** (2021), no. 2, 167–186 Zbl 1515.62137 MR 4350875

Communicated by Adrian Tanasă

Received 30 June 2023; revised 6 January 2025.

Nick Early
School of Natural Sciences, Institute for Advanced Study, 1 Einstein Drive, Princeton, NJ 08540, USA; earlnick@ias.edu

Alheydis Geiger
Max Planck Institute for Mathematics in the Sciences, Inselstrasse 22, 04103 Leipzig, Germany; alheydis.geiger@mis.mpg.de

Marta Panizzut
Department of Mathematics and Statistics, UiT The Arctic University of Norway, Forskningsparken 1, Sykehusvegen 21, 9019 Tromsø, Norway; marta.panizzut@uit.no

Bernd Sturmfels
Max Planck Institute for Mathematics in the Sciences, Inselstrasse 22, 04103 Leipzig, Germany; bernd@mis.mpg.de

Claudia He Yun
Department of Mathematics and Statistics, UiT The Arctic University of Norway, Forskningsparken 1, Sykehusvegen 21, 9019 Tromsø, Norway; he.yun@uit.no